

X. Nanomanipulation with the Atomic Force Microscope

X.1 Introduction

The Scanning Probe Microscope (SPM) provides a direct window into the nanoscale world, and is one of the primary tools that are making possible the current development of nanoscience and nanoengineering. The first type of SPM was the Scanning Tunneling Microscope (STM), invented at the IBM Zürich laboratory by Binnig and Rohrer [Binnig *et al.* 1982], who received the Nobel Prize for it only a few years later (1986). The STM provided for the first time the ability to image individual atoms and small molecules, and it is still widely used, especially to study the physics of metals and semiconductors. Much of the STM work is conducted in ultra high vacuum (UHV) and often at low temperatures. The STM main drawback is the need for conductive samples, which rules out many of its potential applications in biology and other important areas.

The next instrument to be developed in the SPM family was the Atomic Force Microscope (AFM), sometimes also called Scanning Force Microscope [Binnig *et al.* 1986]. The AFM has become the most popular type of SPM because, unlike the STM, it can be used with non-conductive samples, and therefore has broad applicability. Today, there are many other types of SPMs. All of these instruments scan a surface with a sharp tip (with apex radius on the order of a few nm), placed very close to the surface (sometimes at distances ~ 1 nm), and measure the interaction between tip and surface. For example, STMs measure the tunneling current between tip and sample, and AFMs measure interatomic forces—see Section X.2 below for a lengthier discussion of SPM principles.

It was noticed from the beginnings of SPM work that scanning a sample with the tip often modified the sample. This was initially considered undesirable, but researchers soon recognized that the ability to modify a surface could be exploited for nanolithography and nanomanipulation. In SPM nanolithography one writes lines and other structures directly on a surface by using the SPM tip. A well-known technique is called local oxidation, first demonstrated by passing an STM tip in air over a surface of hydrogen-passivated silicon [Dagata *et al.* 1990]. Other materials can be used, as well as a conductive AFM tip in lieu of an STM [Snow & Campbell 1995]. Another STM method involves removing atoms from a silicon surface by applying voltage pulses to the tip [Salling & Lagally 1994]. Lines as narrow as a silicon dimer have been produced by this method. Lithography by material deposition, as opposed to material removal, has also been demonstrated in early work. For example, in [Becker *et al.* 1987] atomic-level structures of germanium were deposited on a Ge surface in UHV by pulsing the voltage on an STM tip, whereas in [Mamin *et al.* 1990] gold clusters were deposited on a gold surface also by applying voltage pulses to the STM tip, but in air and at room temperature. Many other SPM nanolithography approaches have been demonstrated—see [Wiesendanger 1994] for a survey of early work.

More recently, several other SPM nanolithographic techniques have been developed. Some examples follow. Dip Pen Nanolithography [Piner *et al.* 1999] involves depositing

material on a surface much like one writes with a pen on paper. A pen (the AFM tip) is inked by dipping it into a reservoir containing the material to be deposited, and then it is moved to the desired locations on the sample. As the tip approaches the sample, a capillary meniscus is formed, which drives the material onto the sample. Other approaches are discussed *e.g.* in [Diaz *et al.* 2001, Mesquida & Stemmer 2001, Sun & Legget 2002, Davis *et al.* 2003, Garino *et al.* 2003, Takeda *et al.* 2003]. For a recent review see [Wouters & Schubert 2004].

Nanomanipulation is defined in this chapter as the motion of nanoscale objects from one position to another on a sample under external control. Precise, high-resolution nanolithography shares with nanomanipulation the need for accurately positioning the tip on the sample. This is a challenging issue, which we will discuss later in this article.

Given the atomic resolution achieved by SPM imaging, one would expect also that atoms might be moved individually. This is indeed the case, and it was demonstrated in the early 1990s [Eigler & Schweitzer 1990]. At the IBM Almadén laboratory, Eigler's group has been able to precisely position xenon atoms on a nickel surface, platinum atoms on platinum, carbon monoxide molecules on platinum [Stroscio & Eigler 1991], iron on copper [Crommie *et al.* 1993], and so on, by using a sliding, or dragging process. The tip is brought sufficiently close to an adsorbed atom for the attractive forces to prevail over the resistance to lateral motion. The tip then moves over the surface, and the atom moves along with it. Tip withdrawal leaves the atom in its new position.

Eigler also has succeeded in transferring to and from an STM tip xenon atoms on platinum and nickel, platinum on platinum, and benzene molecules. This was done by approaching the atoms or molecules with the tip until contact (or near contact) was established. In addition, xenon atoms on nickel were transferred to the tip by applying a voltage pulse to the tip. All of Eigler's work cited above has been done in ultra high vacuum (UHV) at 4 K.

Avouris group, at the IBM Yorktown laboratory, and Aono's group in Japan have transferred silicon atoms between an STM tip and a surface in UHV at room temperature, by applying voltage bias pulses to the tip [Lyo & Avouris 1991, Uchida *et al.* 1993].

Atomic manipulation with SPMs continues to be studied today and is providing new insights into nanoscience. For example, in the late 1990s, Rieder's group in Berlin conducted a series of experiments in which they showed that xenon atoms can be pushed and pulled across a copper surface, in UHV and at low temperature, and that the tunnel current during the motion has distinct signatures that correspond to the pushing and pulling modes [Bartels *et al.* 1997]. As an example of very recent work, a NIST group has showed that a cobalt atom can be moved on a copper surface by exciting it electronically with an STM tip in UHV and at low temperature [Stroscio *et al.* 2006].

Molecules have been arranged into prescribed patterns at room temperature by Gimzewski's group at IBM's Zürich laboratory (now at UCLA). They push molecules at room temperature in UHV by using an STM. They have succeeded in pushing porphyrin

molecules on copper [Jung *et al.* 1996], and they have arranged bucky balls (*i.e.*, C_{60}) in a linear pattern, using an atomic step in the copper substrate as a guide [Cuberes *et al.* 1996]. They approach the molecules, change the voltage and current values of the STM so as to bring the tip closer to the sample than in imaging mode, and push with the feedback on. C_{60} molecules on silicon also have been pushed with an STM in UHV at room temperature by Maruno and co-workers in Japan [Maruno *et al.* 1993], and Beton and co-workers in the U.K. [Beton *et al.* 1995]. In Maruno's approach the STM tip is brought closer to the surface than in normal imaging mode, and then scan across a rectangular region with the feedback (essentially) turned off. This may cause probe crashes. In Beton's approach the tip also is brought close to the surface, but the scan is done with the feedback on and a high value for the tunneling current; the success rate is low.

It should be clear from this brief review, which is not meant to be exhaustive, that much work has been done in nanomanipulation and related topics. In this article our focus is on manipulation by using AFMs, in air or a liquid, of objects such as nanoparticles or nanowires, which are larger than atoms or small molecules. The remainder of the chapter is organized as follows. First we address in some detail the principles of operation of the AFM, and the spatial uncertainties associated with the instrument. Next we present various protocols for moving nanoobjects with the AFM tip and discuss research aimed at building nanoassemblies. Section X.4 addresses systems for nanomanipulation, both interactive and automated. We draw conclusions in a final section.

Before we embark on the main discussion of this chapter, we point out that SPM manipulation is not the only way of positioning nanoobjects on a surface. A variety of other approaches has been reported in the literature, using principles from optics, magnetics, electrophoresis and dielectrophoresis, which are beyond the scope of this chapter. The pros and cons of these other approaches are not fully understood. For example, optical, laser traps are normally used to move micrometer-sized particles, but they can also manipulate smaller objects. They can achieve 3-D (three-dimensional) positioning, unlike AFMs, but cannot resolve objects which are at a distance significantly below the wavelength radiation used, which is typically in the hundreds of nanometers.

X.2 Principles of Operation of the AFM

X.2.1 The Instrument and its Modes of Operation

The AFM links the macroworld inhabited by users, computers and displays to the nanoworld of the sample by using a microscopic *cantilever* that reacts to the interatomic forces between its sharp *tip* and the sample. Cantilevers are typically built from silicon or silicon nitride by using MEMS (microelectromechanical systems) mass fabrication techniques. They have typical dimensions on the order of $100 \times 20 \times 5 \mu\text{m}$. Tips are built at one of the ends of the cantilevers and are usually pyramidal or conical with apex diameters on the order of 10-50 nm. The tip apex has dimensions comparable to those of the sample's features and can interact with them effectively.

Fig. X.2.1.1 shows diagrammatically the interaction between atoms in the tip and in the sample. The main forces involved are the long-range electrostatic force (if the tip or sample are charged), the relatively short-range van der Waals force, the capillary force (when working in ambient air, which always contains some humidity), and the repulsive force that arises when contact is established [Israelachvili 1992]. The cantilever bends under the action of these forces, and its deflection is usually measured by an optical system, as shown in Fig X.2.1.2. Laser light bounces off the back of the cantilever, opposite to the tip, and is collected in the two halves of a photodetector. In the AFM jargon, the electrical signals output from the two photodetector halves are called A and B, and the differential signal is called $A - B$. For zero deflection and a calibrated instrument, the differential signal from the detector is also zero, and in general $A - B$ is approximately proportional to the cantilever deflection. The force between tip and sample is simply the product of the measured deflection and the cantilever's spring constant k , which can be determined in several ways [Burnham *et al.* 2003].

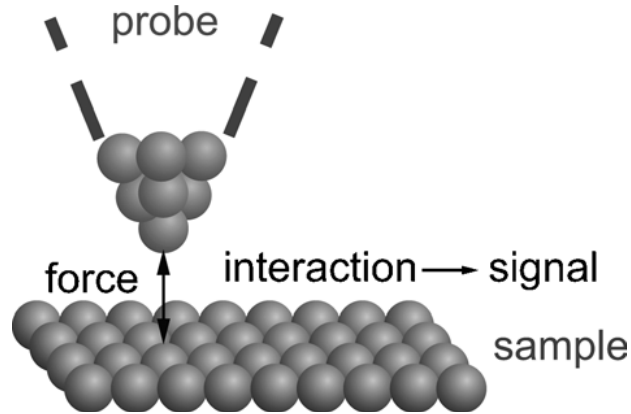


Fig. X.2.1.1 – Tip sample atomic interactions.

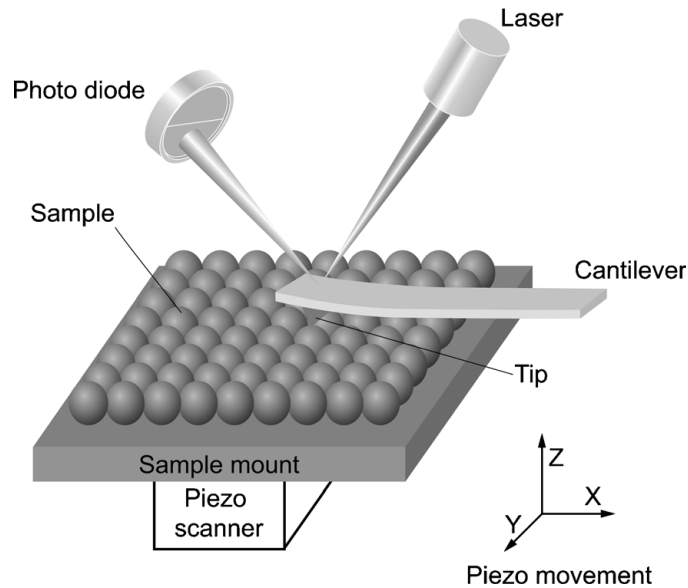


Fig. X.2.1.2 – Optical detection of cantilever deflection.

Relative motion between the tip and the sample is accomplished by means of a *scanner*, which consists of piezoelectric actuators capable of imparting x , y , z displacements to the tip or, more commonly, to the sample. (We assume that the sample is on the x , y horizontal plane, and the tip is approximately aligned with the z axis.) Piezo drives react quickly and are very precise, but require high voltages on the order of 100-200 V, and have a small range of motion. They also are highly nonlinear, as we will discuss later.

In *contact mode* operation, the tip first moves in z until it contacts the sample and a desired value of the tip-sample force, called the *force setpoint*, is achieved. Then it scans the sample by moving in x , y in a raster fashion, while moving also in z under feedback control to maintain a constant force. The feedback circuitry is driven by the deviation (or error) between the (scaled) photodetector signal $A - B$ and the force setpoint. Suppose that the tip moves in straight line along the x direction, at a constant y . When it encounters a change of height Δz of the sample, the scanner must move the sample by the same Δz in the z direction to maintain the contact force (*i.e.*, cantilever deflection). Therefore, the amount of motion of the scanner in z at point x gives us exactly the height of the surface $z(x)$, usually called the *topography* of the surface. Now we move the tip back to the beginning of the line, increment y by Δy and scan again in the x direction. If we do this for a large number of y values we obtain a series of *line scans* that closely approximate the surface of the sample $z(x, y)$. In this example, x is called the *fast scan* direction, and y the *slow scan* direction. In practice, line scan signals are sampled (perhaps after some time-averaging) and discretized, and the output signal becomes a series of values $z(x_i, y_j)$, often called *pixel* values, since the output is a digital image. These images are normally displayed by encoding the height values z as intensities. Of course, other display options are also available, such as perspective images that provide a better feel for the three-dimensional structure of the sample, and so on. A typical AFM image contains 256x256 pixels. For this resolution and a square scan of size 1x1 μm , pixels are $\sim 4 \times 4$ nm, which is a rather large size. Therefore, very small scan sizes are necessary for precise operations.

In contact mode, essentially, the tip is pushed against the sample and dragged across it. This may damage the sample and the tip, and may dislodge nanoobjects from the surface on which they are deposited, thereby making it impossible to image them. An alternative mode of AFM operation that avoids the drawbacks of contact mode and is kinder to the tip and sample is the *dynamic* mode, also known by other designations such as non-contact, tapping, intermittent-contact, AC, and oscillatory. Here the cantilever is vibrated at a frequency near its resonant frequency, which is typically on the order of 100-300 kHz in air and 1-30 kHz in water. The vibration is usually generated by a dedicated piezo drive installed at the base of the cantilever. The piezo moves the cantilever endpoint opposite to the tip up and down at a frequency near resonance, and the vibration is mechanically amplified by the cantilever, resulting in a much larger amplitude of oscillation at the tip. Alternatively, the cantilever can be coated with a magnetic material and oscillated by means of an external electromagnet. This is usually called *MAC* mode (for magnetic AC), and does not require operation near the resonance frequency since it does not rely on mechanical amplification.

The amplitude of the vibration at the output of the photodetector is computed, typically by a lock-in amplifier or an analog or digital demodulation technique, and compared with an amplitude setpoint A_{set} . Feedback circuitry drive the z piezo and adjust the vertical displacement to keep the amplitude constant—see Fig. X.2.1.3.

The principles of dynamic mode operation may be explained by approximating the vibrating tip with a harmonic oscillator in a nonlinear force field, as follows. Suppose initially that the tip is at some distance z_0 to the sample, with a force $F(z_0)$ between tip and sample. Then, the following equation of motion must be satisfied:

$$m\ddot{z}_0 + c\dot{z}_0 + kz_0 = F(z_0),$$

where m is the effective mass, c is the damping coefficient, k is the spring constant, and the dots denote derivatives with respect to time. Now, consider deviations from this point that are small compared to the tip-sample distance. Denote by z the deviation from the value z_0 . The equation of motion may now be written as

$$m(\ddot{z}_0 + \ddot{z}) + c(\dot{z}_0 + \dot{z}) + k(z_0 + z) = F(z_0 + z).$$

Subtracting the two previous equations, expanding F in Taylor series and keeping only the first term yields

$$m\ddot{z} + c\dot{z} + kz = zF'(z_0),$$

where F' denotes the derivative of F with respect to z . This equation may be written as

$$m\ddot{z} + c\dot{z} + k'z = 0,$$

where

$$k' = k - F'(z_0).$$

This means that small deviations of the cantilever satisfy the equations of motion of a simple harmonic oscillator with a spring constant k' , which depends on the actual spring constant of the cantilever and the gradient of the tip-sample force at the equilibrium point. Therefore, the resonance frequency changes from its initial value to

$$\omega'_0 = \sqrt{k'/m}.$$

When the cantilever is at a large distance from the sample, the interaction forces between the two are negligible, the cantilever has a resonance frequency f_{res} corresponding to its spring constant k , and has a resonance curve (amplitude vs. frequency) as shown by the red curve in Fig. X.2.1.4.

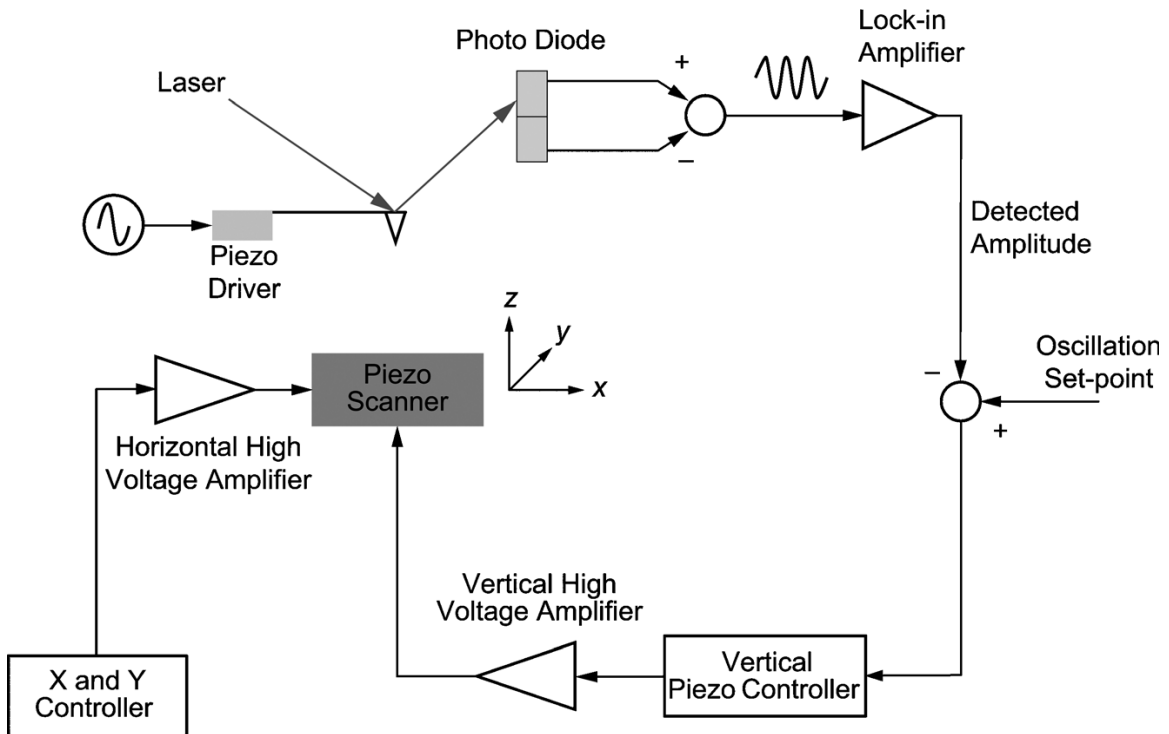


Fig. X.2.1.3 – Schematic of AFM dynamic mode system.

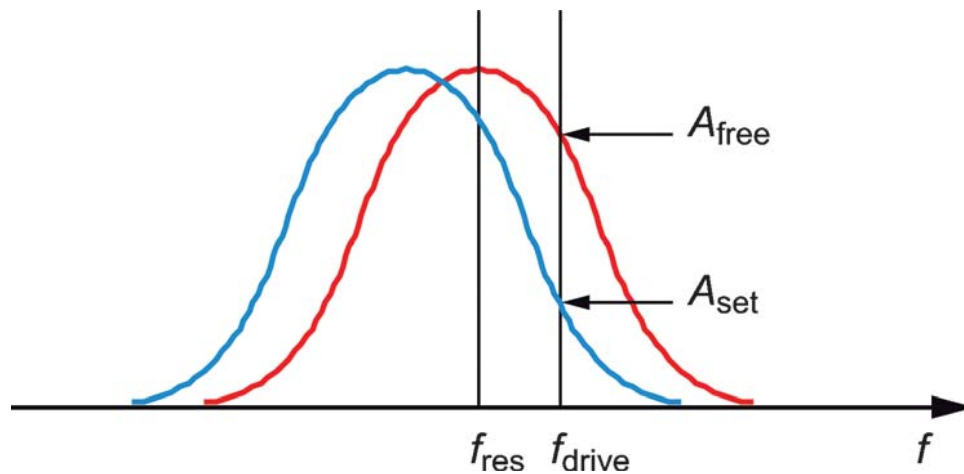


Fig. X.2.1.4 – Amplitude vs. frequency curves when the cantilever is at a large distance from the sample (red) and when the distance is smaller so that there is significant interaction and a concomitant shift of resonance frequency (blue).

Suppose now that we drive the cantilever at a frequency f_{drive} , which generally is near f_{res} . If the tip is sufficiently far from the sample for the interaction force to be negligible, $F=0$, the cantilever oscillates with the frequency f_{drive} and an amplitude A_{free} that we can read directly from the resonance curve. This is called the *free amplitude*. Now we specify an amplitude setpoint, smaller than A_{free} . For the cantilever to oscillate at this amplitude, the resonance curve must shift as shown by the blue curve in the figure. Therefore, the

feedback system must move the cantilever closer to the sample until the force gradient is such that the spring constant and corresponding resonant frequency shift appropriately. We see that the DC, or average, position of the cantilever is controlled in a rather indirect manner, via the f_{drive} , A_{free} , and A_{set} parameters. (The free amplitude essentially scales the resonance curve.) A_{set} is usually specified as a percentage of A_{free} . Typical values of A_{set} are on the order of 80%. Lower setpoints imply large damping, which means that a considerable amount of the cantilever's oscillation energy is being transferred to the sample. In essence, we are tapping hard on the sample, and this is usually undesirable.

The theory just presented is simple and provides an intuitive understanding of the dynamic mode operation. Unfortunately, it is predicated on a linearization about an operating point, and is valid only for small oscillation amplitudes. Usually, however, the AFM is operated with a setpoint that implies a relatively large amplitude and causes the tip to hit ("tap" on) the surface of the sample at the lower part of each oscillation cycle. The actual behavior of the cantilever when tapping is involved is rather complicated—see *e.g.* [Garcia & San Paulo 1999, 2000]. But in normal imaging conditions the oscillation amplitude varies approximately linearly with the DC tip position, as shown in Fig. X.2.1.5. Note that such A-d (amplitude-distance) curves vary from cantilever to cantilever and depend on several parameters.

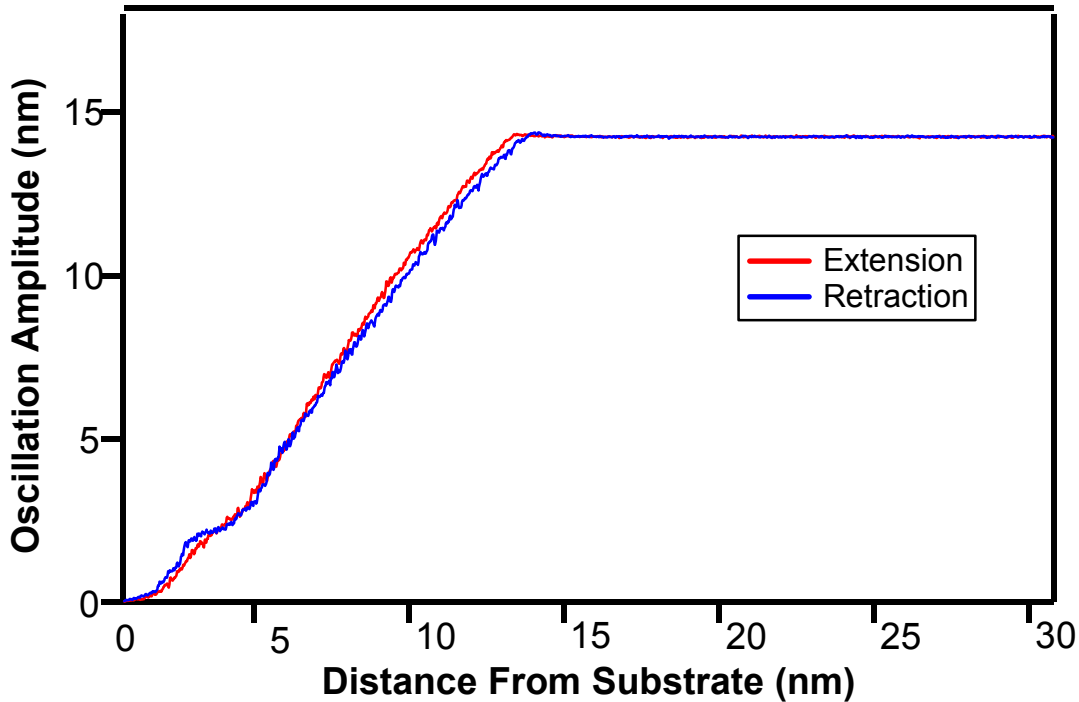


Fig. X.2.1.5 – Experimental amplitude-distance curve obtained with the MFP-3D AFM (Asylum Research). Cantilever resonance frequency 240.654 kHz, drive frequency 240.556 kHz, spring constant ~ 25 N/m, free amplitude 14.2 nm. The zero point for the distance from the surface was inferred by extrapolating the A-d curve to the zero amplitude point.

The feedback circuitry in dynamic mode maintain a constant amplitude, and therefore a constant distance to the sample. (Here we are assuming that the sample is of a homogeneous material, or at least that the tip-sample forces do not vary over the sample's extent.) Scanning the tip over the sample in dynamic mode produces a topographic image of the sample. There are other modes of AFM operation, but the two discussed above are the most common and important.

More information on AFM theory and practice are available for example in [Sarid 1994, Waser 2003, Meyer *et al.* 2004]

X.2.2 Spatial Uncertainties

Let us now turn our attention to the sources of positional errors in AFM operation. These give rise to spatial uncertainty and are important for accurate imaging and especially for nanomanipulation. User intervention is normally used to compensate for spatial uncertainties in nanomanipulation, but extensive user interaction is slow and labor intensive, and therefore is severely limited in the complexity of structures it can construct. Automatic operation is highly desirable but cannot be accomplished without compensating for spatial uncertainties, as we will show below. Compensation techniques are described later in this chapter, in Section X.4.2.

We noted earlier that the output of a line scan along the x direction is the topography $z(x)$. In the actual implementation this is not quite true. If no error compensation is used, the output is $V_z(V_x)$, where V_z and V_x are the voltages applied to the z and x piezos. In an ideal situation these voltages would be linearly related to the piezo extensions, and the signals $V_z(V_x)$ and $z(x)$ would coincide modulo scale factors. But in practice they don't.

There are many nonlinearities involved. Some of these are normally taken into account by AFM vendors' hardware and software, for example, non-linearities in the voltage-extension relationship for the piezos, coupling between the different axes of motion, and so on. The most pernicious are drift, creep and hysteresis. As far as we know, at the time of this writing (2006), drift is not adequately compensated for in any commercial instrument, and creep and hysteresis are negligible only in top of the line AFMs that have feedback control for the x , y directions, and whose controller noise r.m.s. is under 1 nm. The vast majority of AFMs in use today either have no x , y feedback or have noise levels on their feedback circuitry that are too large for precise lithography and manipulation. Open-loop operation with a small scan size (*e.g.* $1 \times 1 \mu\text{m}$) is preferable for nanomanipulation operations with such instruments.

Drift is caused by changes of temperature in an instrument made from several materials with different coefficients of expansion. At the very low temperatures often used for atomic manipulation the effects are negligible, but at room temperature they can be quite large. Fig. X.2.2.1 shows four AFM images of gold nanoparticles with 15 nm diameters, taken at successive times, 8 min apart. The particles appear to be moving, but in reality they are fixed on the substrate surface. The piezos are driven by the same voltage signals in all the panels of the figure, and have the same extensions, but the position of the tip

relative to the sample is the sum of the piezo extension and the drift, and therefore changes with time. Experimental observations in our lab indicate that drift is a translation with speeds on the order of 0.01 to 0.1 nm/s. The drift velocity remains approximately constant for several minutes, and then appears to change randomly to another value.

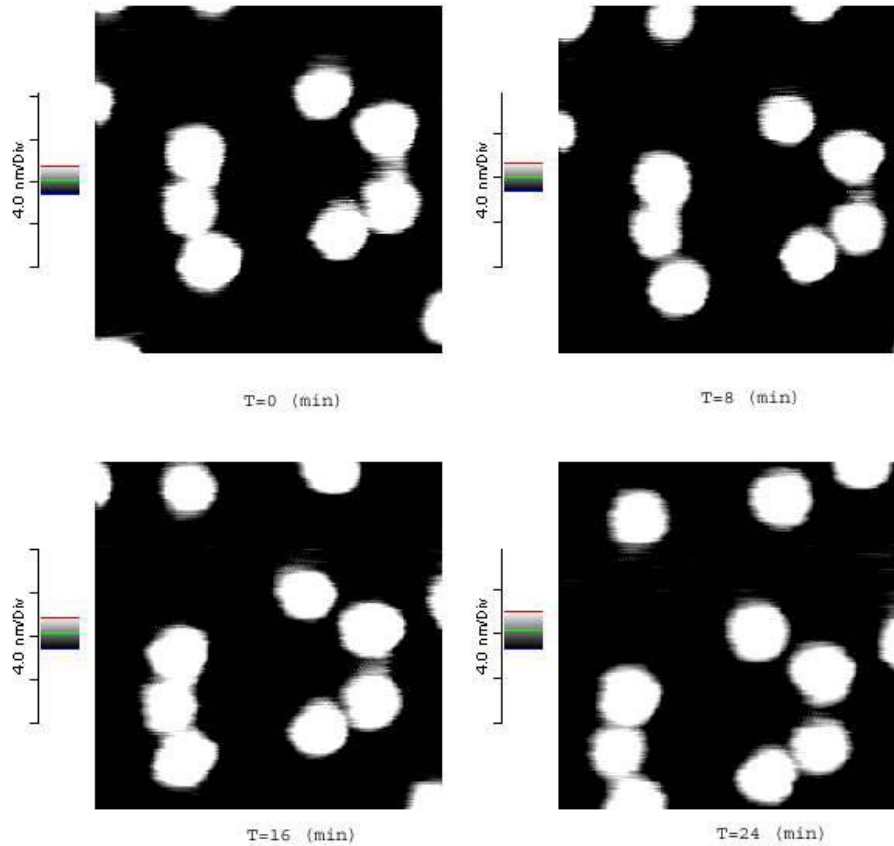


Fig. X.2.2.1 – Successive images taken at 8 min intervals showing the effects of thermal drift. Gold nanoparticles with nominal diameter 15 nm on mica coated with poly-L-lysine, 1 Hz scan rate, Autoprobe CP-R AFM (Veeco).

Suppose now that we were trying to manipulate a large set of nanoparticles similar to those in Fig. X.2.2.1, and that the manipulation operations would take a total time of 1 hour. Assuming an average drift velocity of 0.05 nm/s, the total drift after 1 hour would be 180 nm. If we relied on the original images and did not compensate for drift, it is clear that as time went by we would completely miss most of the 15 nm particles.

After drift, creep is another major source of spatial uncertainty in AFMs. A piezo actuator commanded to move by a certain distance first responds very quickly and moves by ~ 70-90% of the commanded distance, and then slowly “creeps” to the final position—see Fig. X.2.2.2. Creep is especially noticeable for large motions. Successive images of the (nominally) same area taken after a large tip displacement show an apparent motion of the features in the area. The effects of creep can last several minutes and are sufficiently

large to foil manipulation attempts, especially for small particles with dimensions on the order of 10 nm. Creep can be avoided by waiting for several minutes after any large tip motion, but this is obviously a very inefficient approach.

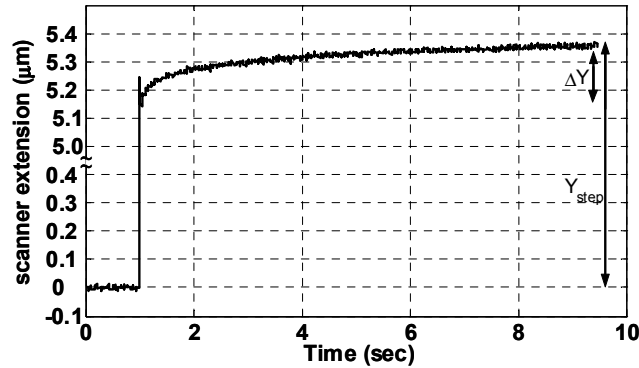


Fig. X.2.2.2 – Experimental curve showing a scanner response to a 5.4 μm step function.

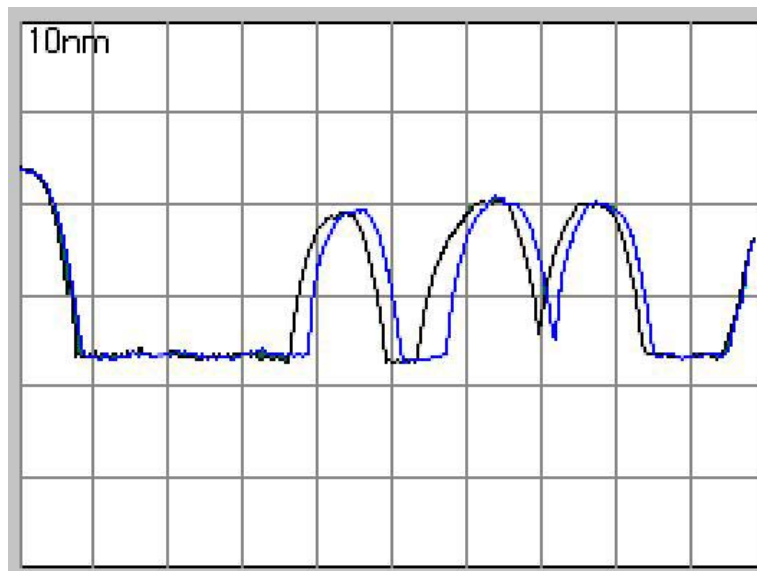


Fig. X.2.2.3 – Hysteresis effects. Left-to-right vs. right-to-left single-line scans of 15 nm Au particles on mica. Scan size 100 nm.

Hysteresis is also present in piezo actuators and has non-negligible effects—see Fig. X.2.2.3. Hysteresis is a nonlinear process with memory. The extension of a piezo depends not only on the currently applied voltage, but also on past extremal values.

Finally, the images of the features that appear in a topography scan differ from the actual physical features in the sample because of tip effects. The tip functions as a low-pass filter, and broadens the images. To a first approximation, the image's lateral dimensions

of a feature equal the true dimensions plus the tip diameter. Algorithms are known for combating this effect [Villarubia 1994]. Note that the vertical dimensions of a feature's image are not affected by the tip's dimensions.

Compensation of spatial uncertainties due to drift, creep and hysteresis in AFMs will be discussed later, in Section X.4.2, in the context of automated nanomanipulation.

X.3 Nanomanipulation: Principles and Approaches

X.3.1 LMR Nanomanipulation by Pushing

Here we discuss the approach to nanomanipulation that has been under development at USC's Laboratory for Molecular Robotics (LMR) over the last decade. It was first presented at the 4th International Conference on Nanometer-Scale Science & Technology, Beijing, P. R. China, September 8-12, 1996, and later reported in a string of papers [Baur *et al.* 1997, 1998, Bugacov *et al.* 1999, Requicha *et al.* 1998, 2001, Resch *et al.* 1998a]. Other approaches are considered in the next subsection.

We begin by preparing a sample with nanoparticles or other structures to be manipulated. A typical sample consists of a mica surface coated with poly-L-lysine, on which we deposit Au nanoparticles. The coating is needed because freshly cleaved mica is negatively charged, and so are the nanoparticles; the poly-L-lysine attaches to the mica and offers a positively-charged surface to the nanoparticles. We have also used other surfaces such as (oxidized) silicon, glass and ITO (indium tin oxide), other coatings such as silane layers [Resch *et al.* 2001], other particles such as latex, silver or CdSe, and rods or wires of various kinds. We typically manipulate particles with diameters between 5 and 30 nm, but have occasionally moved particles as small as 2 nm and as large as 100 nm. In all cases the structures to be moved are weakly attached to the underlying surfaces and cannot be imaged by contact mode AFM. We image them in dynamic mode, apply a flattening procedure to remove any potential surface tilt, and then proceed with the manipulation. The bulk of our experiments have been conducted in ambient air at room temperature and without humidity control, but we also have demonstrated manipulation in a liquid environment [Resch *et al.* 2000]. We use stiff cantilevers, with spring constants > 10 N/m.

The nanomanipulation process is very simple. We move in a straight line with an oscillating tip towards the center of a particle and, before reaching the particle, turn off the z feedback. We turn the feedback on when we reach the desired end of the particle trajectory. With the feedback off, the tip does not move up to keep constant distance to the sample when it encounters a nanoparticle. Rather, it hits the particle and pushes it. We use the same dynamic AFM parameters for pushing as for imaging, but sometimes we force the tip to approach the surface by applying directly a command to move by Δz immediately after turning off the feedback.

Fig. X.3.1.1 shows experimental data acquired during a pushing operation for a 15 nm Au particle on mica. The two vertical dashed lines indicate the points where the feedback is

turned off and on. The top trace (A) is simply the topography signal acquired by a single line scan in dynamic mode. The next trace (B) is the topography signal during the push. The topography signal is flat while the feedback is off because the tip does not move up and down to follow the sample topography. Observe that as soon as the feedback is turned back on we immediately get a non-null topography signal that indicates that the tip was somewhat below the top of the particle at the end of the manipulation. We conclude from these data that the tip is pushing the particle forward rather than dragging it behind itself.

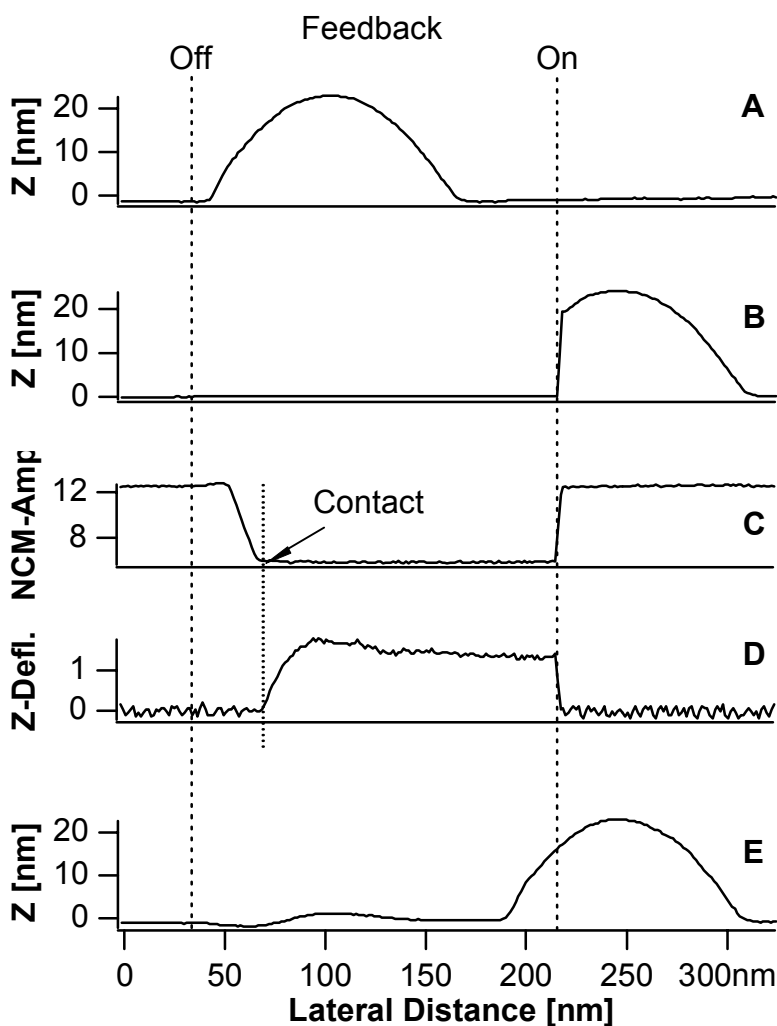


Fig. X.3.1.1 – Data acquired during a manipulation operation. (A) Dynamic-mode single line scan image of the particle before manipulation. (B) Topography signal during the push. (C) Vibration amplitude during the push. (D) Average position of the antilever during the push. (E) Image of the particle after the manipulation. AutoProbe AFM, 15 nm Au particles on mica with poly-L-lysine, cantilevers with (nominal) spring constant 13 N/m.

Trace C shows the amplitude of the vibration during the manipulation. The amplitude is constant at the setpoint value when the feedback is on, but it decreases as the tip approaches the particle with the feedback off, and eventually reaches zero and stays at zero for the remainder of the push. At the same time that the amplitude decreases, the average (DC) value of the cantilever deflection increases and then reaches an approximately constant level—trace D in the figure. Finally, trace E is a single line scan after the push.

We interpret the data in Fig. X.3.1.1 as follows. When the tip approaches the particle with the feedback off, it starts to exchange energy with the particle and the vibration amplitude decreases, much like in standard A-d curves (see Section X.2.1). When the vibration goes to zero, the tip touches the particle, and remains in contact with it until the feedback is turned on. While the tip contacts the particle the cantilever starts to “climb” the particle, and the DC deflection increases. When enough force is exerted on the particle for it to overcome the surface adhesion forces, the particle moves, and the deflection (and hence the force) remains approximately constant. Our experiments reveal that there is a deflection (or force) threshold above which the particle moves.

For successful pushing, the trajectory has to pass close to the center of the particle. Here the spatial uncertainties discussed in Section X.2.2 are a major source of problems. We address these problems in the interactive version of our Probe Control Software (PCS) as follows. The user draws a line over the image and instructs the AFM to scan along that line and output the corresponding topography signal. The user moves the line over (or perhaps near) the particle to be pushed until he or she detects the maximum height of the particle—see Fig. X.3.1.2. This indicates that the line is going through the center of the particle. Usually this is several nm away from the apparent center because of drift and other spatial uncertainties. After the center is found, the user sets two points along the trajectory for turning the feedback off and on, and instructs the AFM to proceed with the push. The result can be assessed immediately by looking at the single line scan after the push—see trace E in Fig. X.3.1.1.

The amplitude and deflection signals—see traces C and D in Fig X.3.1.1—are useful to assess whether a pushing operation is proceeding normally. For example, we have observed experimentally that when we “loose” a particle (*i.e.*, when it does not move as far as specified) the deflection drops to zero prematurely. In principle, one could monitor the amplitude and deflection signals while pushing and, for example, stop and locate the particle when the signals are not as expected. In practice, however, this may require substantial modifications to the controller, if decisions are to be made automatically based on this information while the manipulation operation is taking place.

How reliably can particles be moved by the LMR approach? Fig. X.3.1.3 attempts to answer this question. Observe that operations in which the commanded motion is below 50 nm are very successful, whereas for distances ~ 80 nm the actual and desired displacements of the particles begin to differ considerably. The reasons why pushing over large distances is unsuccessful are not fully understood.

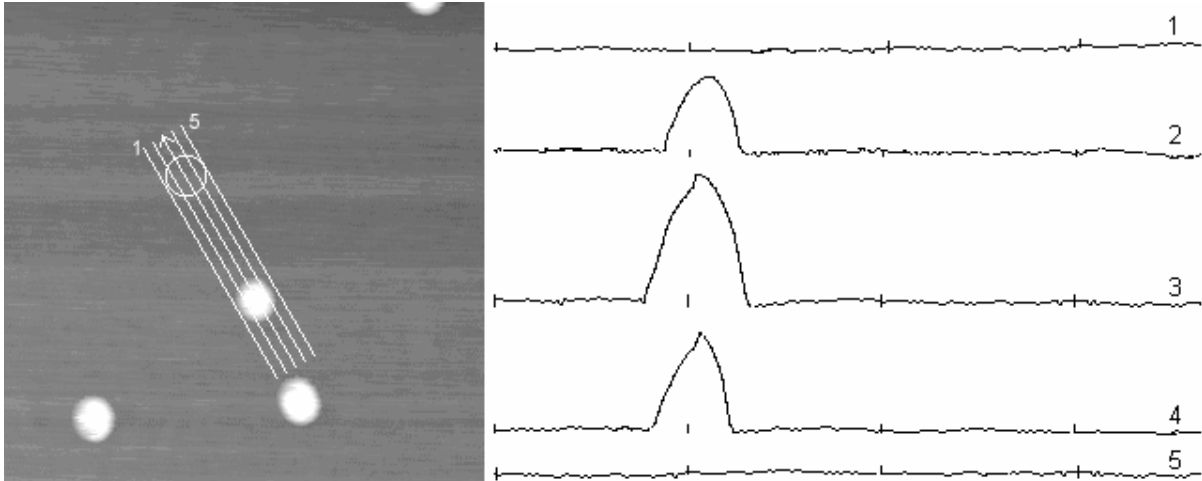


Fig. X.3.1.2 – Interactive search for the center of a particle with single line scans. Line 3 has the largest peak and is chosen as trajectory for the pushing operation.

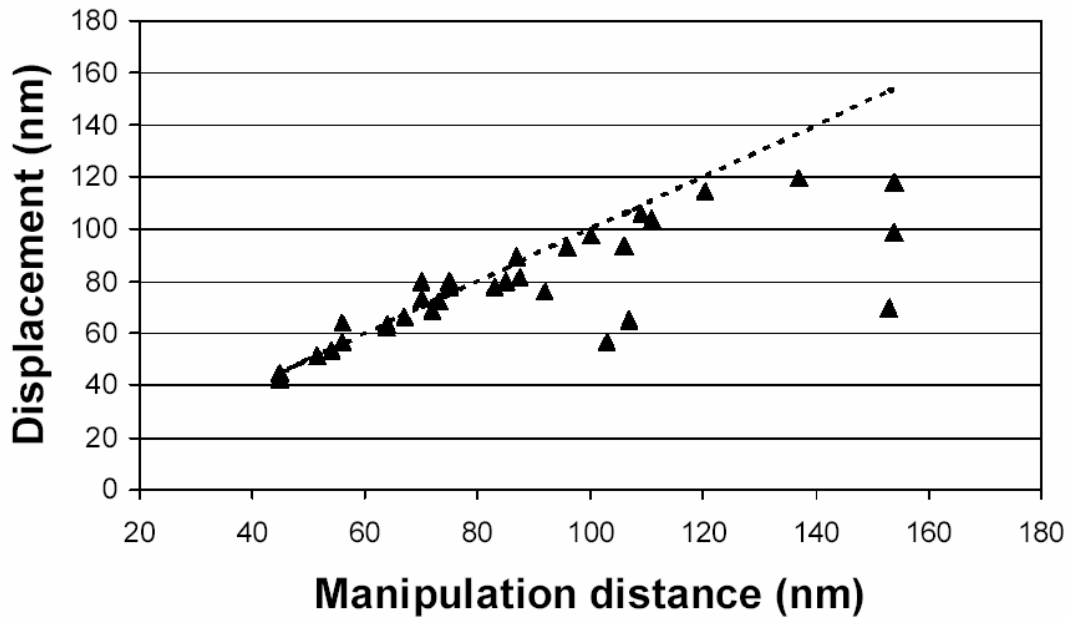


Fig. X.3.1.3 – Reliability plot, showing the actual distance a particle moved as a function of the commanded manipulation distance. AutoProbe CP-R, 15 nm Au particles on mica, interactive pushing. The dashed line corresponds to perfect pushing, with equal actual and commanded displacements.

X.3.2 Other Approaches

At the LMR we have experimented with several other approaches to pushing nanoparticles. We had occasional success with all of these approaches, but did not achieve reproducible, controlled manipulation. The reliability of these protocols has been until now much lower than that of the standard method discussed in the previous subsection. Here is a short description of these various protocols. They all begin with imaging in dynamic mode and finding a particle's center interactively, as discussed earlier.

- As the tip approaches the particle, instead of turning the feedback off and on, change the amplitude setpoint so that the tip gets closer to the surface.
- Move towards the particle while tapping hard on the substrate and then turn the feedback off and on. This appears to induce a “lateral push”, in which the cantilever deflection does not increase as in the standard pushing protocol of the previous subsection.
- Approach the particle while moving in a zig-zag pattern, in a direction normal to the desired trajectory and with the feedback off. This appears to simulate pushing with a linear edge rather than a round tip, and has been reported in [Requicha 2003, Taylor *et al.* 1997].

The first published reports that demonstrated manipulation of nanoparticles with the AFM came from Purdue University in the U.S. [Schaefer *et al.* 1995] and the University of Lund in Sweden [Junno *et al.* 1995]. The Purdue group pushed 10-20 nm gold clusters on graphite or WSe₂ substrates with an AFM, in a nitrogen environment at room temperature [Schaefer *et al.* 1995]. They image with non-contact AFM, but then stop the cantilever oscillation, approach the substrate until contact, disable the feedback, and push. Samuelson's group at the University of Lund succeeded in pushing gallium arsenide (GaAs) nanoparticles of sizes in the order of 30 nm on a GaAs substrate at room temperature in air [Junno *et al.* 1995]. They use an AFM in non-contact mode, approach the particles, disable the *z* feedback and push. This is the protocol investigated in detail later on by the LMR, and discussed in the previous subsection. Essentially the same protocol is used in [Martin *et al.* 1998] to push Ag nanoparticles. They observe that the vibration amplitude decreases as the particle is approached, and then essentially vanishes during pushing, which agrees with the findings in our own laboratory.

Lieber's group at Harvard has moved nanocrystals of molybdenum oxide (MoO₃) on a molybdenum disulfide (MoS₂) surface in a nitrogen environment by using a series of contact AFM scans with large force setpoints [Sheehan & Lieber 1996]. The nanoManipulator group at the University of North Carolina at Chapel Hill moves particles by increasing the contact force, under user control through a haptic device [Guthold *et al.* 2000]. Sitti's group reports manipulation of Au-coated latex particles with nominal diameters 242 and 484 nm on a Si substrate with accuracies on the order of 20-30 nm [Sitti & Hashimoto 2000]. First, they move the tip until it contacts the surface, and then move it horizontally to a point near the particle, and up by a predetermined amount. Next, they move against the particle using feedback to maintain either constant height or

constant force on the particle. In constant-height pushing, the force signal exhibits several characteristic signatures that may be interpreted as signifying that the particle is sliding, rolling or rotating. Constant-force pushing is equivalent to contact-mode manipulation. Xi's group at Michigan State University has demonstrated pushing of latex nanoparticles with 110 nm diameters on a polycarbonate surface by two methods [Li *et al.* 2003]. The first consists of scanning in contact mode with a high force. The second disables the feedback and moves the tip open loop along a computed trajectory based on a model of the surface acquired by a previous scan. This requires an accurate model of the surface.

Theil Hansen and coworkers moved Fe particles on a GaAs substrate by approaching a particle in dynamic mode, switching to contact mode and pushing with the feedback on [Theil Hansen *et al.* 1998]. This has the advantage that the pushing force can be controlled by the AFM. However, switching modes is a non-trivial operation that can cause damaging transients. (In the AutoProbe CP-R AFM that we use routinely for nanomanipulation at LMR, such a switch is not allowed by the vendor's software.) Furthermore, switching from tapping to contact mode implies that the tip in contact mode does not touch the same point of the surface it was tapping on, because the cantilever normally is not horizontal—see Fig. X.3.2.1.

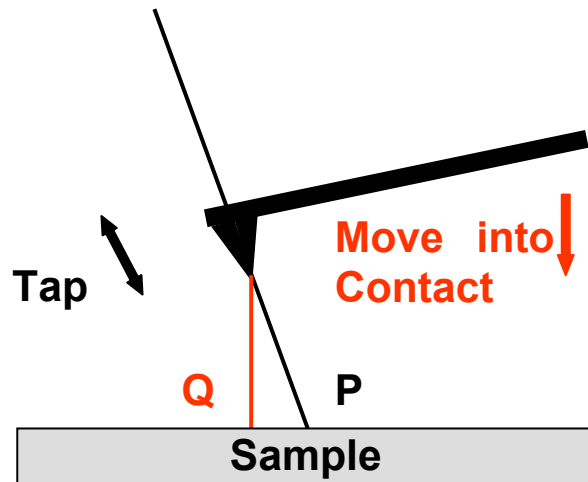


Fig. X.3.2.1 – A cantilever is initially tapping on a sample at point P. When the AFM is switched into contact mode and the vibration stops, the tip must approach the sample to maintain contact. However, the contact will be at point Q, not P.

The LMR and related protocols are essentially “open-loop”, because it is virtually impossible to incorporate the force sensed by the cantilever into a feedback loop during actuation for commercial AFMs. For example, in the AutoProbe CP-R we are completely “blind” during a pushing operation. We can record the force (deflection) signal while pushing, but cannot do anything with it until the motion stops. To do otherwise would require a major change to the controller. On the other hand, it is not difficult to make the force signal available for visualization in interactive pushing, and several research groups have reported such capabilities. By developing their own controllers, Sitti and co-workers have been able to use the force signal during pushing, primarily to determine when an

operation should be stopped because it is not going to succeed. When the tip-particle force drops to zero the particle is no longer being pushed. One should stop the motion, locate the particle and schedule a new operation to deliver it to its target position.

The AFM is both an imaging device and a manipulator but not both simultaneously. For example, it would be useful to see a particle while it is being pushed, but this cannot be done solely with an AFM. An interesting approach that provides real-time visualization consists of operating the AFM within the chamber of a Scanning Electron Microscope (SEM), or sometimes a Transmission Electron Microscope (TEM). The motion of the tip can then be monitored by the electron microscope and known techniques for visual feedback developed at larger spatial scales can be deployed [Vikramaditya & Nelson 1997].

The AFM-SEM approach was pioneered by Sato's group for microscopic objects [Sato *et al.* 1995, Miyazaki & Sato 1997], and has been used successfully by several groups [Yu *et al.* 1999, Guthold *et al.* 2000, Dong *et al.* 2001a, Fatikow *et al.* 2006]. In some of this work an AFM cantilever is used as an end effector for a specially-built micromanipulator. Working inside an SEM has its drawbacks: electron microscopes are expensive instruments, they are less precise than AFMs, require more elaborate sample preparation, and normally operate in a vacuum environment, which precludes their use for certain applications, for example, in biology.

All of the work on AFM nanomanipulation discussed above involves essentially pushing objects on a flat surface. Pushing nanoparticles over steps [Baur *et al.* 1998] and onto other particles [Resch *et al.* 1998b] has been demonstrated by our group, but this is a very rudimentary 3-D capability. More sophisticated 3-D tasks would be feasible if there was the equivalent of a macroscopic "pick-and-place" operation for nanoparticles. (Pick-and-place is possible with atoms and small molecules, as noted in the Introduction.) We know of only one report in which nanoparticles are controllably picked up by the AFM tip and then deposited elsewhere [Decossas *et al.* 2003]. They succeed in picking up Si nanocrystals deposited by silane CVD (chemical vapor deposition) on a Si surface. They place the tip in contact with the particle and apply successive voltage pulses of opposite polarity to the AFM tip. The tip is then moved to a target location, lowered until there is contact with the surface, and again a series of pulses are applied. This work requires a dry atmosphere and the experiments were performed in a nitrogen environment. The process appears to have limited reproducibility. Diaz and co-workers report a pick-and-place process that uses redox reactions on the tip to pick up and deposit particles, but they only demonstrate it for large, micrometer scale particles [Diaz *et al.* 2001]. Note that it is not difficult to pick up a nanoobject with a tip, even by just using van der Waals forces. What is very hard to do is to controllably release the object at a target location.

X.3.3 Manipulation and Assembly of Nanostructures

The majority of the experimental work on nanomanipulation has been conducted with nanoparticles. These are simple but interesting nanoobjects because many types of them are available (metallic, semiconducting, magnetic, etc.), they often are monodisperse (i.e.,

have the same size), they can be smaller and more uniform than structures made by other means such as electron-beam lithography, and can be arranged into arbitrary patterns by nanomanipulation. Patterns of nanoparticles may be useful in themselves, or they may serve as templates for constructing other structures [Requicha 1999b]. We present examples of both below.

Fig. X.3.3.1 illustrates the use of particle patterns to store digital information. The particles are located at the nodes of a uniform grid. We interpret the presence of a particle at a node as a digital “1” and its absence as a “0”. Each row of particles represents an ASCII character. From top to bottom, this structure encodes the characters “LMR”. These are 15 nm Au nanoparticles, and the internode distance along a row or column is ~ 100 nm, which corresponds to a density of 10 Gbit/cm². This is considerably higher than the current compact disk (CD) density. By using smaller particles and closer spacing, higher densities are achievable. In addition, this structure is editable, simply by moving the particles.

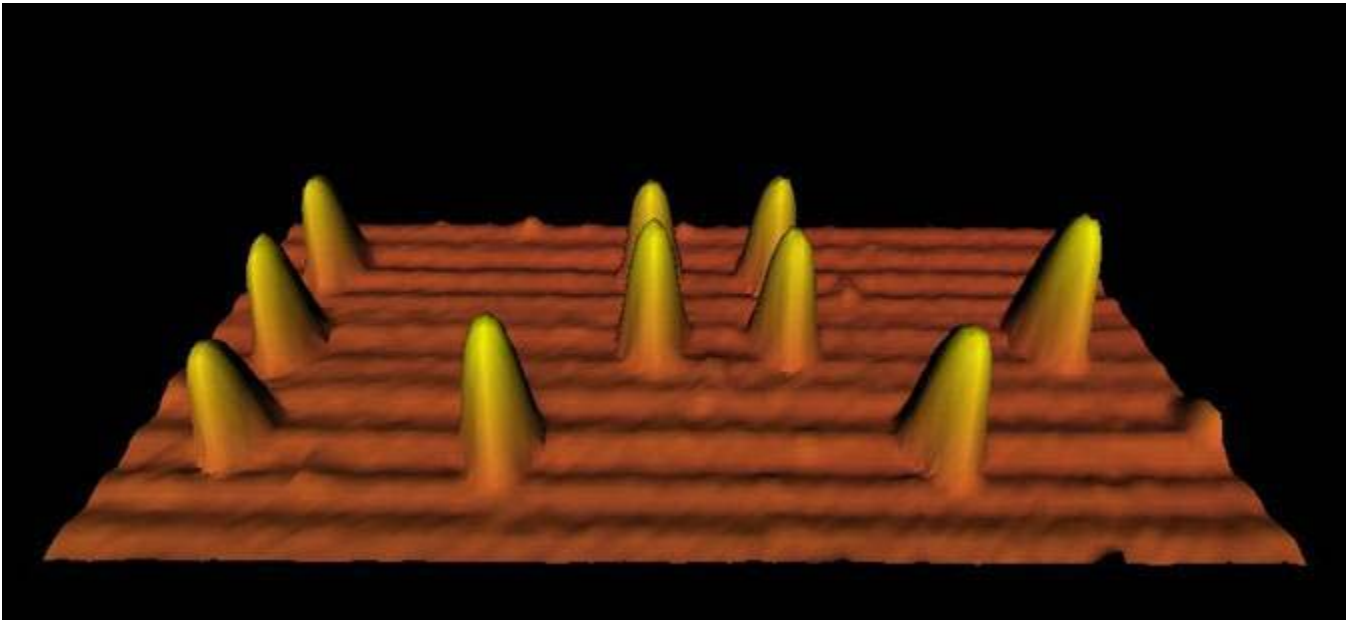


Fig. X.3.3.1 – The ASCII characters “LMR” encoded in the positions of 15 nm Au nanoparticles on mica.

Nanoparticle patterns can also be used as a resist, as shown by research at the University of Konstanz, Germany [Burmeister *et al.* 1998]. They started with a self-assembled regular pattern and deposited material so as to fill the space between the particles. By etching the particles away, they obtained the complement of the original pattern. In a similar vein, a Japanese/English group used regular nanoparticle patterns as templates in a process that involves both etching and growth [Tada *et al.* 1998]. They deposited nanoparticles on a Si substrate and then etched the Si. As the substrate was etched away, reaction products condensed around the nanoparticles and formed regular patterns of pillars with diameters on the order of a few nm. Similar results were obtained in [Lewis

& Ahmed 1999]. Another use of Au nanoparticles as a mask is reported in [Zheng *et al.* 2000], where they demonstrate that the particles can serve as an anti-oxidation mask to prevent the AFM-tip induced oxidation of a modified Si surface. Subsequent etching produces Si nanopillars. In all of these cases, it should be possible to perform similar operations for arbitrary patterns constructed by nanomanipulation. Nanoparticle manipulation may also be an effective way to build templates or molds, for example for imprinting techniques that construct a large number of structures in a parallel fashion by pressing a template against a substrate [Chou *et al.* 1996]. Nanoparticle-based templates can be more uniform and have smaller features than those built by other means such as electron-beam lithography. Applications to template or mold making, however, have not yet been demonstrated.

Nanoparticle manipulation with the AFM has been used to build prototype structures for several nanodevices such as single-electron transistors [Junno *et al.* 1988, Requicha 2003], plasmonic waveguides [Maier *et al.* 2001, 2003], and quantum-dot cellular automata gates [Mokaberi & Requicha 2006].

Most nanoparticles are approximately spherical, although some of the nanoparticles used in the research cited above (*e.g.*, [Junno *et al.* 1995]) are more like “islands”, and have vertical dimensions smaller than their horizontal counterparts. Structures with other shapes have also been nanomanipulated. Rods, wires and tubes have been investigated extensively. They normally require a series of pushes to reach a target position because they tend to rotate. And sometimes they deform or even break, rather than simply move on the surface. At the LMR we have manipulated Au rods with diameters ~ 10 nm and lengths ~ 70 nm deposited on a SiO₂/Si (111) substrate modified with MPMDMS (3-mercaptopropylmethylmethoxysilane) [Hsieh *et al.* 2002]. Xi’s group has demonstrated manipulation of Ag rods with diameters ~ 110 nm on a polycarbonate surface [Chen *et al.* 2006].

Several groups have manipulated carbon nanotubes (CNTs). Avouris and co-workers at the IBM Yorktown laboratories moved multiwall CNTs on a hydrogen-passivated Si surface by using contact mode AFM [Hertel *et al.* 1998]. They also showed that the nanotubes can be bent and cut by the AFM tip. The nanoManipulator group in North Carolina reported rolling and sliding of CNTs on a graphite surface [Falvo *et al.* 1999]. Other work in CNT manipulation include [Dong *et al.* 2001a, 2001b, 2003], [Yu *et al.* 1999] and [Roschier *et al.* 1999], who built a single-electron transistor by manipulating a multiwall CNT so as to connect it to electrodes made by electron-beam lithography. Several of these groups also used the AFM tip to probe the mechanical properties of the CNTs—see *e.g.* [Guthold *et al.* 2000] [Yu *et al.* 1999]. Nanowires can also be manipulated by the AFM. Fig. X.3.3.2 shows on the left a SnO₂ wire with a diameter of ~ 10 nm and a length of ~ 9 μ m, and on the right the result of cutting the wire in two spots and then moving the three smaller wires. The manipulation was done at the LMR by using our standard protocols.

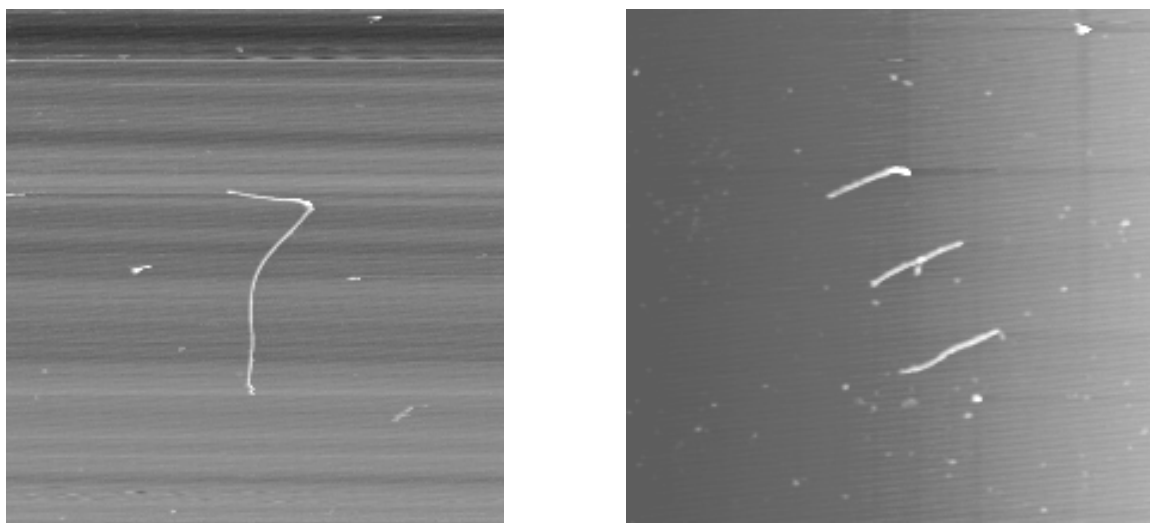


Fig. X.3.3.2 – Cutting a SnO_2 nanowire and making an array with the resulting three pieces by using the AFM tip.

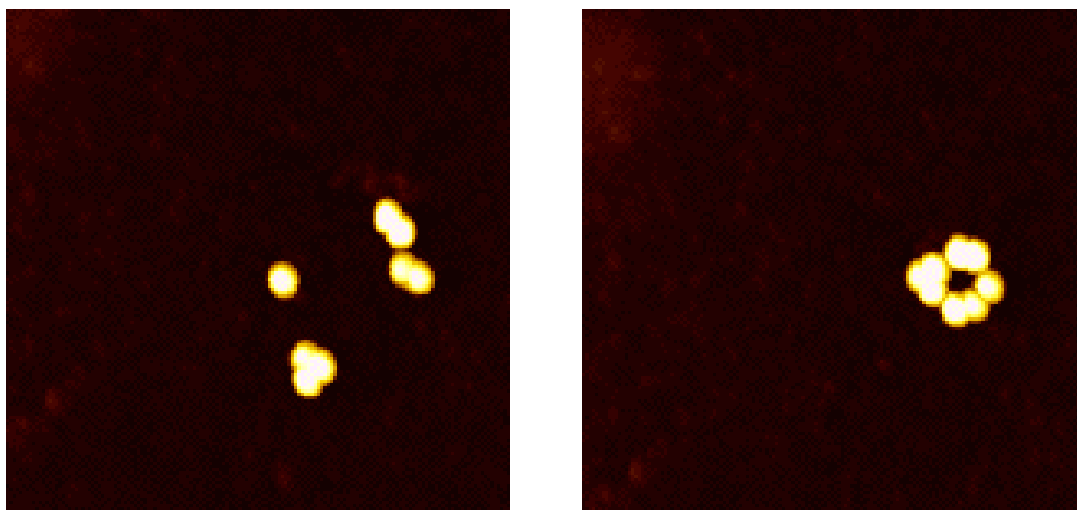


Fig. X.3.3.3 – Hierarchical assembly. Thiolated 27 nm Au nanoparticles on Si coated with poly-L-lysine, 800x800 nm scan size.

For many applications, particles and other nanoscale objects must be linked together to form a single, larger object. Linking may be accomplished by various methods: chemically, by using material deposition, sintering, and “welding”. We showed that Au nanoparticles can be connected chemically by using linkers with thiol functional ends [Resch *et al.* 1999]. This can be done in two ways: (1) the particles are first functionalized with the di-thiols, then deposited and manipulated against one another to form the target structure, or (2) the manipulation is done first and then the thiol treatment is applied. In either case the result appears to be the same. The resulting assemblies can then be manipulated by using the same protocols, and joined to make larger assemblies.

Therefore, we have demonstrated that hierarchical assembly is possible at the nanoscale [Requicha *et al.* 1999]. Fig. X.3.3.3 shows on the left clusters of 2 and 3 particles, which were constructed by manipulating individual particles (initial configuration not shown). On the right is a ring-like structure obtained by moving the clusters on the left.

A different approach is reported in [Meltzer *et al.* 2001]: nanoparticles are manipulated to form a target structure, which is then grown by deposition of additional material. Growth is accomplished essentially by electroless deposition, by immersing the sample in a hydroxylamine seeding solution. Fig. X.3.3.4 illustrates the results. On the top left is a “wire” made by manipulating Au particles, and on the top right is a single line scan through the centerline of the structure, showing that the height of the particles is ~ 8 nm. On the bottom left is the structure after deposition by hydroxylamine seeding, and on the bottom right is a single line scan, which now shows a particle size of ~ 20 nm. The initial structure looks like a continuous wire in the figure but is not mechanically stable; touching it with the tip causes the structure to fall apart. In contrast, the final structure is a solid wire. One disadvantage of this method is that after the seeding the structures can no longer be moved on the substrate surface.

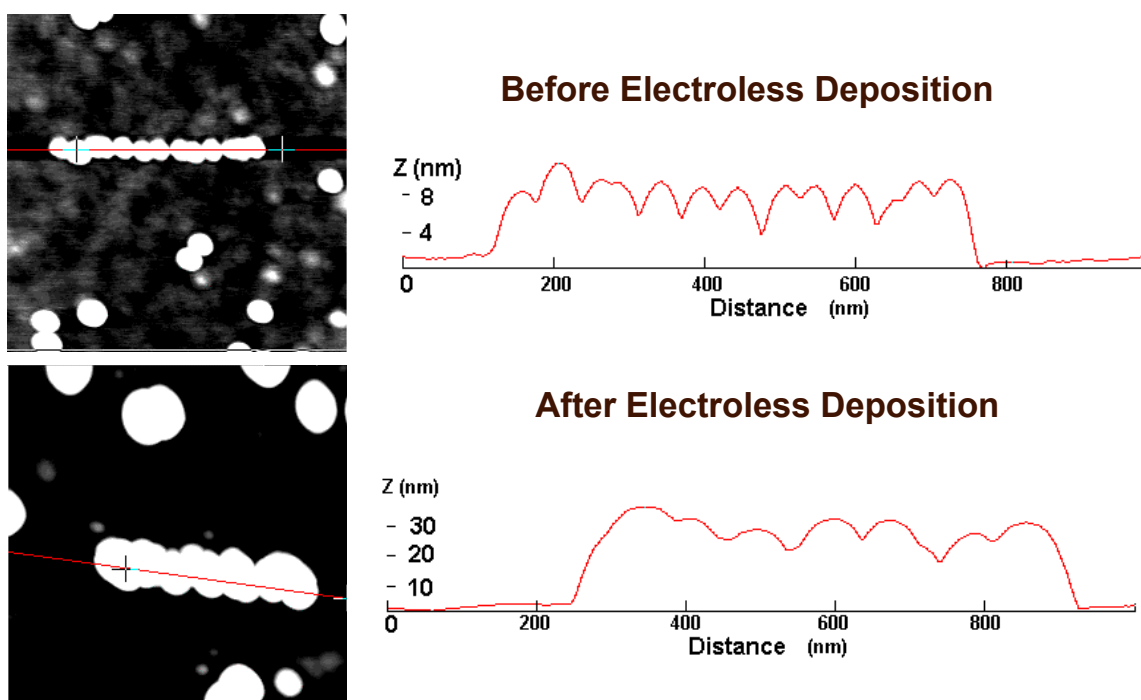


Fig. X.3.3.4 – Linking nanoparticles by hydroxylamine seeding of a template built by manipulation. 8 nm Au particles on Si modified with aminopropyltrimethoxysilane (APTS).

Finally, we have demonstrated an even simpler approach to particle linking, which is based on sintering a structure after its template is built by nanomanipulation [Harel *et al.* 2005]. Fig. X.3.3.5 shows on the left a “wire” built by manipulation of latex particles with 100 nm diameter. On the right is the result of heating the sample at $\sim 160^\circ$ for ~ 10

min. The particles form a contiguous, solid structure. This process works very well for latex particles, but, unfortunately does not appear to be applicable to Au (and perhaps other metallic) particles.

Another interesting approach to joining nanoobjects is “welding”, usually done within an SEM by using the electron beam. Contamination within the SEM chamber usually suffices to generate carbonaceous residues at the beam’s target, and this can be used to link objects such as nanotubes [Yu *et al.* 1999, Dong *et al.* 2001b]. Similar approaches but using an environmental SEM and a field emission SEM are reported, respectively, in [Madsen *et al.* 2003, Dong *et al.* 2003]. Here they “solder” by inducing deposition of conductive materials with the electron beam in the presence of a source of a precursor.

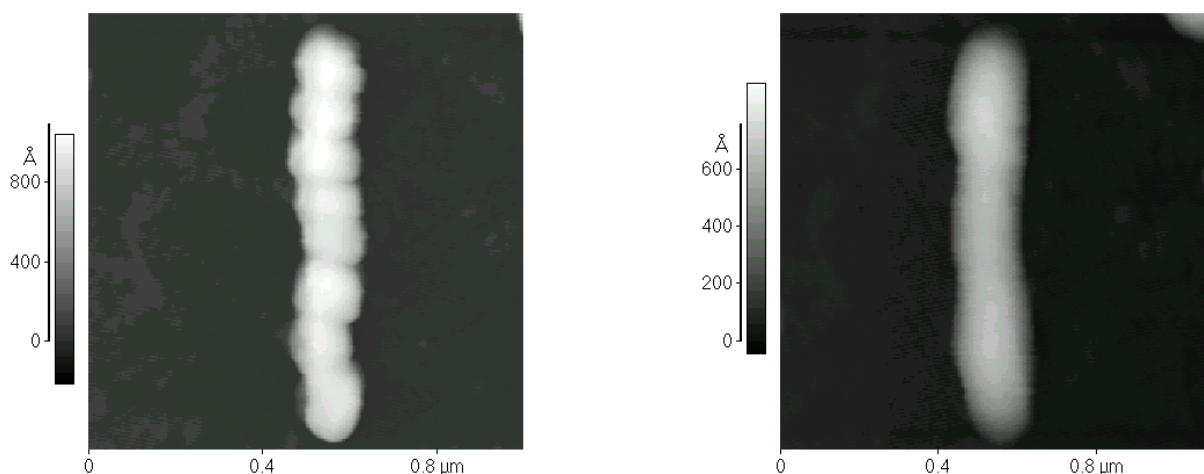


Fig. X.3.3.5 – Linking nanoparticles by sintering a template built by nanomanipulation. 100 nm latex particles on Si.

X.4 Manipulation Systems

X.4.1 Interactive Systems

We discussed briefly in Section X.3.1 the interactive manipulation capabilities of the LMR software. Ours is an unsophisticated system which provides a set of minimal capabilities a user needs to manipulate nanoobjects with the AFM. Since the beginnings of the LMR we have focused on automation—see the next subsection—and therefore did not invest resources in user interfacing.

Much more sophisticated interfaces have been developed by others. Hollis’ group at the IBM Yorktown laboratory (now at Carnegie Mellon University) built an interface to an STM in which the user could drive the tip over the sample by moving a mechanical wrist [Hollis *et al.* 1990]. The z servo signal is fed back to the wrist so that the user feels the topography of the surface as wrist vertical motions. This force, however, is not (a scaled version of) the actual force between tip and sample.

The nanoManipulator group in North Carolina has developed virtual reality user interfaces, first for STMs and then for AFMs [Taylor *et al.* 1993, 1997, Finch *et al.* 1995, Guthold *et al.* 2000]. In the AFM interface a user can either be in imaging or manipulation mode. During imaging, the topographical data collected by the AFM is presented to the user in virtual reality, as a 3-D display. In addition, the user can feel the surface by using a haptic device, as if moving a stylus over a hard surface. Note, however, that the forces felt through the haptic device are not the cantilever-sensed forces, but rather are forces computed by standard virtual reality techniques so as to simulate the feel of a surface that approximates the measured topography of the sample. In the imaging mode, the user haptic input does not control the actual motion of the instrument, but rather the position of a virtual hand over the image of the surface. In contrast, the hand can be used to move the tip over the sample in manipulation mode. As the hand moves in virtual space and the tip moves correspondingly over the sample, the topography data generated by the AFM is used on the fly to compute a planar approximation to the surface. The user feels this approximated surface through the haptic stylus. Although the user does not feel the actual forces sensed by the cantilever, he or she can control the force applied to the sample during manipulation by using a set of knobs.

Sitti and co-workers also implement a virtual reality graphics interface, and add a one degree-of-freedom haptic device [Sitti & Hashimoto 1998, 2000]. Through a bilateral feedback system based on theoretical models of the forces between tip, sample and particle, the user can drive the tip over the sample by using a mouse, while at the same time feeling with the haptic device the forces experienced by the cantilever.

Xi's group has developed an augmented reality system in which cantilever forces are reflected in a haptic device [Li *et al.* 2003a, 2004]. They develop a theoretical model for the interaction forces between tip, object and surface, and use it to compute the position of the tip based on the real-time force being measured. The visual display in a small window around the point of manipulation is updated in real-time to reflect the computed particle position. Thus, a user can follow the (computed) motion of the particle in real time during the manipulation.

X.4.2 Automated Systems

The automatic assembly of nanoobject patterns with the AFM consists of planning and executing the motions required for moving a set of objects from a given initial configuration into a goal configuration. The initial state usually corresponds to nanoobjects randomly dispersed on a surface.

As far as we know, there are only two systems today that are capable of building nanoobject patterns *automatically* by AFM nanomanipulation. One is being developed by Xi's group at Michigan State University, and the other at the LMR [Chen *et al.* 2006, Mokaberi *et al.* 2007]. The two systems use different planning algorithms and pushing protocols. Xi's system addresses at length the issues that arise in nanorod manipulation, and therefore is more general than ours, which focuses on nanoparticles. On the other

hand, the Michigan State system has a more rudimentary drift compensator than ours, and does not compensate for creep or hysteresis, which are important for the manipulation of small objects, with dimensions ~ 10 nm or less. The manipulation tasks demonstrated in [Chen *et al.* 2006] involve objects which are roughly one order of magnitude larger than those we normally manipulate, and the positional errors in the final structures shown in the figures of [Chen *et al.* 2006] also appear to be similarly larger than ours.

In the remainder of this section we describe the LMR automatic manipulation systems, from the top down, starting with high-level planning and ending with the system software architecture.

The input to the planner consists of a specification for a goal assembly of nanoparticles, and an initial arrangement that is obtained by imaging a physical sample with a compensated AFM (compensation is discussed below). In an initial step the planner assigns particles to target locations by using the Hungarian algorithm for bipartite matching, which is optimal [Knuth 1993]. It uses direct, straight-line paths if they are collision free, or indirect paths around obstacles computed by the optimal visibility algorithm [Latombe 1991]. Next, the planner computes a sequence of positioning paths, to connect the locations of the tip at the end of a push (determined in the previous step) and at the beginning of another push. This is done by a greedy algorithm, which sequentially selects the shortest paths. It is sub-optimal but performs well in practice. In a general case collisions between particles may arise. The planner handles collisions by exploiting the fact that all particles are assumed identical. It simulates the sequence of operations previously computed, at each step updating the state of the particle arrangement. If a collision is detected, it swaps operations, and does this recursively because solving one collision problem may generate new ones.

The planner just outlined is the second one we write. Our first planner, developed several years ago [Makaliwe & Requicha 2001], was more complicated and slower, and did not perform better than the current one. However, we abandoned work on planning at that time not because of planner problems, but rather because we could not implement reliably the primitive operation assumed by the planner, which is simply to move from an initial point P to another goal point Q . The spatial uncertainties associated with the AFM—see Section X.2.2—were such that after a few operations we could no longer find the particles and push them without user interaction, and the task could not be completed automatically. We embarked on a research program aimed at compensation of uncertainties, and developed the compensators described briefly below. Details are available in [Mokaberi & Requicha 2004, 2006, 2007]

The drift compensator is based on Kalman filtering, a standard technique in robotics and dynamic systems. We assume a simple (but incorrect) model for the time evolution of the drift. The model can be used to predict future values of the drift, but these values will become increasingly wrong as time goes by, because the model is not perfect. The Kalman equations provide us with means to estimate the prediction error. When this value exceeds a threshold, drift measurements are scheduled, and the measured and predicted values are combined to produce better estimates, again by using the Kalman

equations. A decade-long series of experiments indicates that the drift is accurately approximated as a translation, with a direction and speed that vary slowly. The estimated drift values obtained from the Kalman filter are added as offsets to all the motion commands of the AFM, thus compensating for this translation. Drift measurement techniques require that the AFM tip move on the sample to acquire data. Therefore, manipulation operations must be suspended when a measurement is needed. In contrast, when the filter is in prediction mode the offsets can be calculated very quickly and used to update the coordinates without interrupting the manipulation task.

Creep and hysteresis compensation is achieved through a feedforward scheme. A model for the two phenomena together is constructed as explained below, using a Prandtl-Ishlinskii operator [Mokaberi & Requicha 2007]. This operator has the important property of invertibility. The inverse operator is computed and the desired trajectory is fed to the inverse system. The result is the signal required to drive the AFM piezos so as to follow the goal trajectory, assuming that the model is perfect. The model, of course, is not perfect, but experimental results show that it is sufficiently accurate for obtaining very good results—an order of magnitude decrease on the effects of creep and hysteresis has been verified experimentally. Creep is modeled by a linear term plus a superposition of exponentially decaying terms, with different time constants. Hysteresis is modeled by a superposition of operators which are essentially simple hysteresis loops. The piezo extension is the sum of the values of creep and hysteresis obtained from their models, and can be expressed in terms of a Prandtl-Ishlinskii operator. The combined model depends on several parameters, which can be estimated by analyzing the AFM topography signal for a line scan over a few particles. The line should span the entire region in which the manipulations will take place. The parameters are valid as long as the scan size of the AFM is not changed, and can be computed rapidly by running the tip back and forth a few times with the compensator on. Details may be found in [Mokaberi & Requicha 2007].

Running both compensators together results in a software-compensated AFM with sufficiently low spatial uncertainties to provide a reliable implementation of the most basic robotic primitive “Move from point P to point Q ” on the sample. However, this is not sufficient to reliably push particles between arbitrary points because long pushes tend to be unreliable—see Fig. X.3.1.3. Therefore, we break down any long pushing trajectory into smaller segments, currently ~ 30 nm long. Having a reliable pushing routine, the output of the high-level planner can now be executed also with high reliability.

Now that we have discussed the high-level planner and its primitive commands, let us turn our attention to the software needed to implement the system. We found in the beginnings of the LMR, in 1994, that commercial AFM software was designed for imaging and not suitable for manipulation. Therefore we designed and implemented a manipulation system, called Probe Control Software (PCS), running on top of the vendor-supplied Application Programming Interface (API) [Baur *et al.* 1997]. It was implemented on AutoProbe AFMs (Park Scientific Instruments, which later on became Thermomicroscopes and now Veeco), which to our knowledge were the only instruments sold with an available API. PCS evolved as time went by, and was the workhorse for the

interactive manipulation research in our laboratory until recently. Research often moves in unpredictable ways, and we found that the ability to easily modify the software was fundamental to our experimental work. Unfortunately, the API was written for a 16-bit Windows system, which is far from being convenient to program. We concluded that we were spending too much time fighting an inhospitable programming environment and launched a re-write of the whole system, which has been “completed” recently. (We find that research software is in a permanent state of flux.)

The new system is called PyPCS, for Python PCS. It is written in C++ and Python, which is a scripting language that greatly facilitates program development. For example, new modules may be added to the system without the need to recompile and link the whole system. PyPCS has a client-server architecture. The server is written in C++ for 16-bit Windows and runs in the PC that controls the instrument. The client is written in Python, communicates with the server via standard interprocess communication primitives, and may run in the AFM PC or in any computer that is connected to it by Ethernet [Arbuckle *et al.* 2006].

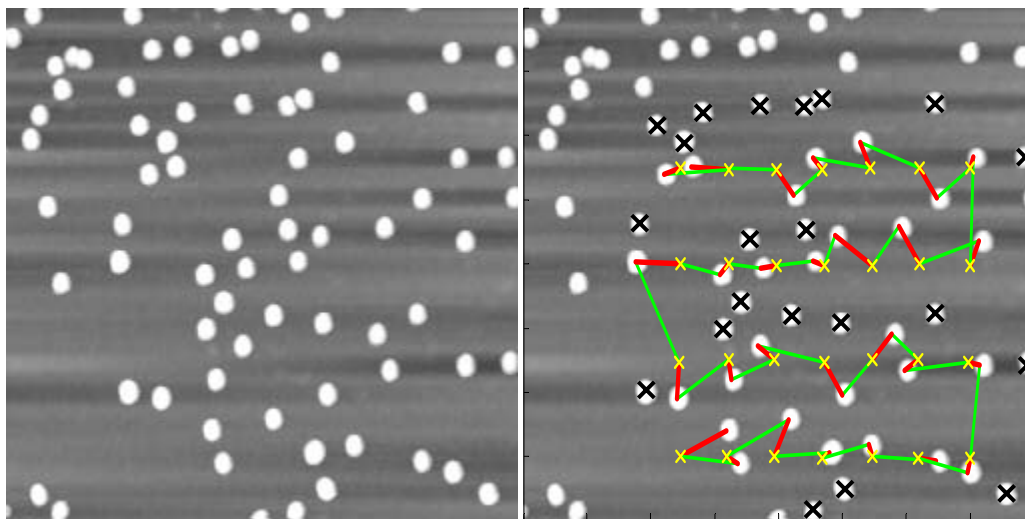


Fig. X.4.2.1 – Left: Initial state. Right: Goal state (yellow) and planner output superposed on the initial image, showing pushing paths (red) and positioning paths (green). 15 nm Au particles on mica.

We conclude this section with a complete example, including planning and execution in the AFM. Fig. X.4.2.1 shows on the left panel the initial random dispersion of nanoparticles on the sample. On the right is the goal configuration (yellow crosses) plus the result of planning, with the pushing paths in red, and the positioning paths between pushes in green. The particles marked with a black cross are extraneous and should be removed from the area where the pattern is being built. (This is also done automatically.) Fig. X.4.2.2 shows on the left the result of executing the plan. On the right is the result of another similar operation also performed automatically. The pattern on the right of Fig. X.4.2.2 represents a different encoding of ASCII characters into nanoparticle positions—

compare with Fig. X.3.3.1. Here a particle on the top row of each 2-row group signifies a ‘1’ and a particle on the bottom row signifies a ‘0’. The 4 groups of 2 rows read ‘NANO’ in ASCII. This encoding uses twice as many particles as that of Fig. X.3.3.1 but has an interesting advantage: editing the stored data amounts simply to pushing particles up or down by a fixed amount, and could be achieved very efficiently by an AFM with a multi-tip array with spacing equal to that of the particle grid—see [Requicha 1999a] and the discussion in the next section. The patterns shown in Fig. X.4.2.2 were built in a few minutes with the automated system. They would take at least one day of work by a skilled user if they had been built with our interactive system.

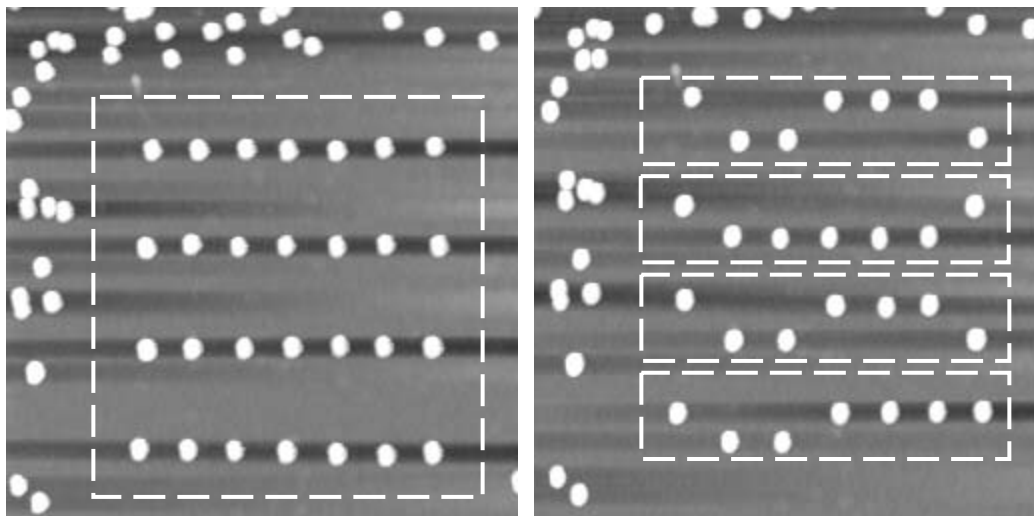


Fig. X.4.2.2 – Left: Result of the execution of the plan of Fig. X.4.2.8. Right: An additional task, also planned and executed automatically.

X.5 Conclusion and Outlook

Manipulation with the AFM of nanoscale objects with dimensions $\sim 5\text{-}100$ nm has been under study for over a decade, and is now routinely performed in several laboratories. Nevertheless, some basic questions remain unanswered. For example, how far off center can we hit a particle for it to be pushed reliably? How high above the surface can we strike a particle for it to move? Does the size of a particle matter? Do the shape and size of a tip matter? Why do particles fall off the desired trajectories? What is the force threshold needed to move a particle? Are there preferred directions of motion? For a given surface, coating, nanoparticle, cantilever and environmental conditions, can we predict which operational parameters, if any, will result in reliable manipulation? And we could go on. In short, we lack a predictive understanding of the manipulation process, especially an understanding grounded on measurable parameters. However, there is enough experimental evidence on certain materials and systems for us to successfully complete non-trivial manipulation tasks, as shown in this chapter.

Nanomanipulation has been used until now for demonstrations or to prototype new devices. It is a useful prototyping tool because it can be used to build devices that cannot

be made otherwise, and it greatly facilitates parametric studies. For example, the effect of spatial errors on a given device can be investigated by moving one of its constituent particles and recording the associated functional changes. The complexity of the structures built by nanomanipulation has been severely restricted by the sheer amount of labor and time needed to construct them interactively. Automated systems such as those described in this chapter are beginning to appear, and may significantly impact what can be done by nanomanipulation. It is fair to say, though, that a “killer app” has not yet been found for nanomanipulation. A high value, low volume application seems most appropriate, because, even with automated operation, nanomanipulation with the AFM is a serial and relatively slow process, not very suitable for mass production. Perhaps repair of fabrication masks and other high cost devices will be an important application in the future.

Another technical advance that may have a strong impact on nanomanipulation is the development of instruments with multiple tips. There are currently several research efforts aimed at producing multi-tip arrays, but they tend to be unusable for manipulation because they do not provide individual control of height (z) for each tip—see *e.g.* [Vettiger *et al.* 2002]. Furthermore, whereas efficient algorithms for nanolithography with multi-tip arrays are known [Requicha 1999a, Arbuckle & Requicha 2003], manipulation tasks are inherently more difficult because of registration problems between tips and particles. The tips are normally arranged in a regular array, while the particles are initially randomly dispersed, and when a tip is positioned near a particle for pushing it, the other tips are unlikely to be in positions where they can push other particles. If this happens, a multi-tip array will be no faster than a single tip.

In summary, much has been learned about nanomanipulation with AFMs, and new automated systems are a breakthrough improvement over their traditional, interactive counterparts, but we still lack a deep, predictive understanding of the manipulation phenomena, as well as a convincing demonstration of economic viability for practical applications. Massively parallel operation by using multi-tip arrays may be the next breakthrough.

Acknowledgment and Disclaimer

The LMR work on nanotechnology was supported in part by the NSF Grants EIA-98-71775, IIS-99-87977, EIA-01-21141, DMI-02-09678 and Cooperative Agreement CCR-01-20778; and the Okawa Foundation.

I would like to thank my LMR faculty colleagues, postdocs and students, too many to mention here, who did much of the LMR work reported in this chapter and from whom I learned much over the last decade. I wish to single out the students who built the probe control software who made possible all of our work on nanomanipulation. They were Cenk Gazen, who started it all, Nick Montoya who extended and maintained PCS for a couple of years, Jon Kelly, who wrote the first version of PyPCS, Babak Mokaberi, who built the drift, creep and hysteresis compensators, Dan Arbuckle, who is the architect of the current version of PyPCS, which integrates the old PCS with Mokaberi’s work, and

Jaehong Yun, who did the high level planning software and, with Arbuckle, has integrated it into PyPCS.

An exhaustive bibliography on nanomanipulation and related topics is beyond the scope of this Chapter. In many cases I have attempted to cite the pioneering works on specific subjects but I may have failed to acknowledge some of them. I offer my apologies to the colleagues whom I may not have cited, or whose work I may have misinterpreted. There is simply too much research in this area for me to be able to keep up with all of it.

References

[Arbuckle & Requicha 2003] D. J. Arbuckle and A. A. G. Requicha, “Massively parallel scanning probe nanolithography”, *Proc. 3rd IEEE Int’l Conf. on Nanotechnology*, S. Francisco, CA, pp. 72-74, August 12-14, 2003.

[Arbuckle *et al.* 2006] D. J. Arbuckle, J. Kelly and A. A. G. Requicha, “A high-level nanomanipulation control framework”, *Proc. Int’l Advanced Robotics Programme (IARP) Workshop on Micro and Nano Robotics*, Paris, France, October 23-24, 2006.

[Bartels *et al.* 1997] L. Bartels, G. Meyer and K.-H. Rieder, “Basic steps of lateral manipulation of single atoms and diatomic clusters with a scanning tunneling microscope tip”, *Physical Review Letters*, Vol. 79, No. 4, pp. 697-700, 28 July 1997.

[Baur *et al.* 1997] C. Baur, B. C. Gazen, B. Koel, T. R. Ramachandran, A. A. G. Requicha and L. Zini, “Robotic nanomanipulation with a scanning probe microscope in a networked computing environment”, *J. Vacuum Science & Technology B*, Vol. 15, No. 4, pp. 1577-1580, July/August 1997.

[Baur *et al.* 1998] C. Baur, A. Bugacov, B. E. Koel, A. Madhukar, N. Montoya, T. R. Ramachandran, A. A. G. Requicha, R. Resch, and P. Will, “Nanoparticle manipulation by mechanical pushing: underlying phenomena and real-time monitoring”, *Nanotechnology*, Vol. 9, No. 4, pp. 360-364, December 1998.

[Becker *et al.* 1987] R. S. Becker, J. A. Golovchenko and B. S. Swartzentruber, “Atomic-scale surface modifications using a tunneling microscope”, *Nature*, Vol. 325, No. 6103, pp. 419-421, 29 January 1987.

[Beton *et al.* 1995] P. H. Beton, A. W. Dunn and P. Moriarty, “Manipulation of C₆₀ molecules on a Si surface”, *Applied Physics Letters*, Vol. 67, No. 8, pp. 1075-1077, 21 August 1995.

[Binnig *et al.* 1982] G. Binnig, H. Rohrer, Ch. Gerber and E. Weibel, “Surface studies by scanning tunneling microscopy”, *Physical Review Letters*, Vol. 49, No. 1, pp. 57-61, 5 July 1982.

[Binnig *et al.* 1986] G. Binnig, C. F. Quate and Ch. Gerber, “Atomic force microscope”, *Physical Review Letters*, Vol. 56, No. 9, pp. 931-933, 3 March 1986.

[Bugacov *et al.* 1999] A. Bugacov, R. Resch, C. Baur, N. Montoya, K. Woronowicz, A. Papson, B. E. Koel, A. A. G. Requicha and P. Will, “Measuring the tip-sample separation in dynamic force microscopy”, *Probe Microscopy*, Vol. 1, pp. 345-354, 1999.

[Burmeister *et al.* 1998] F. Burmeister, C. Schäfle, B. Keilhofer, C. Bechinger, J. Boneberg and P. Leiderer, “From mesoscopic to nanoscopic structures: lithography with colloid monolayers”, *Advanced Materials*, Vol. 10, No. 6, pp. 495-497, 1988.

[Burnham *et al.* 2003] N. A. Burnham, X. Chen, C. S. Hodges, G. A. Matei, E. J. Thoreson, C. J. Roberts, M. C. Davies and S. J. B. Tendler, “Comparison of calibration methods for atomic-force microscopy cantilevers”, *Nanotechnology*, Vol. 14, No. 1, pp. 1-6, January 2003.

[Chen *et al.* 2006] H. Chen, N. Xi and G. Li, “CAD-guided automated nanoassembly using atomic force microscopy-based nanorobotics”, *IEEE Trans. on Automation Science & Engineering*, Vol. 3, No. 3, pp. 208-217, July 2006.

[Chou *et al.* 1996] S. Y. Chou, P. R. Krauss and P. J. Renstrom, “Imprint lithography with 25-nanometer resolution”, *Science*, Vol. 272, No. 5258, pp. 85-87, 5 April 1996.

[Crommie *et al.* 1993] M. F. Crommie, C. P. Lutz and D. M. Eigler, “Confinement of electrons to quantum corrals on a metal surface”, *Science*, Vol. 262, No. 5131, pp. 218-220, 8 October 1993.

[Cuberes *et al.* 1996] M. T. Cuberes, R. R. Schlittler and J. K. Gimzewski, “Room-temperature repositioning of individual C₆₀ molecules at Cu steps: operation of a molecular counting device”, *Applied Physics Letters*, Vol. 69, No. 20, pp. 3016-3018, 11 November 1996.

[Dagata *et al.* 1990] J. A. Dagata, J. Schneir, H. H. Harary, C. J. Evans, M. T. Postek and J. Bennett, “Modification of hydrogen-passivated silicon by a scanning tunneling microscope operating in air”, *Applied Physics Letters*, Vol. 56, No. 10, pp. 2001-2003, 14 May 1990.

[Davis *et al.* 2003] Z. J. Davis, G. Abadal, O. Hansen, X. Borisé, N. Barniol, F. Pérez-Murano and A. Boisen “AFM lithography of aluminum for fabrication of nanomechanical systems”, *Ultramicroscopy*, Vol. 97, Nos. 1-4, pp. 467-472, October-November 2003.

[Decossas *et al.* 2003] S. Decossas, F. Mazen, T. Baron, G. Brémond and A. Souifi, “Atomic force microscopy nanomanipulation of silicon nanocrystals for nanodevice fabrication”, *Nanotechnology*, Vol. 14, No. 12, pp. 1272-1278, December 2003.

[Diaz *et al.* 2001] D. J. Diaz, J. E. Hudson, G. D. Storrier, H. D. Abruna, N. Sundararajan and C. K. Ober, "Lithographic applications of redox probe microscopy", *Langmuir*, Vol. 17, No. 19, pp. 5932-5938, 18 September 2001.

[Dong *et al.* 2001a] L. Dong, F. Arai and T. Fukuda, "3D nanorobotic manipulation of multi-walled carbon nanotubes", *Proc. IEEE Int'l Conf. on Robotics & Automation*, Seoul, S. Korea, pp. 632-637, May 21-26, 2001.

[Dong *et al.* 2001b] L. X. Dong, F. Arai and T. Fukuda, "Three-dimensional nanoassembly of multi-walled carbon nanotubes through nanorobotic manipulations by using electron-beam induced deposition", *Proc. 1st IEEE Int'l Conf. on Nanotechnology*, Maui, HI, pp. 93-98, October 28-30, 2001.

[Dong *et al.* 2003] L. Dong, F. Arai, M. Nakajima, P. Liu and T. Fukuda, "Nanotube devices fabricated in a nano laboratory", *Proc. IEEE Int'l Conf. on Robotics & Automation*, Taipei, Taiwan, pp. 3624-3629, September 24-29, 2003.

[Eigler & Schweitzer 1990] D. M. Eigler and E. K. Schweizer, "Positioning single atoms with a scanning tunneling microscope", *Nature*, Vol. 344, No. 6266, pp. 524-526, 5 April 1990.

[Falvo *et al.* 1999] M. R. Falvo, R. H. Taylor II, A. Helser, V. Chi, F. P. Brooks, Jr., S. Washburn and R. Superfine, "Nanometre-scale rolling and sliding of carbon nanotubes", *Nature*, Vol. 397, No. 6716, pp. 236-238, 21 January 1999.

[Fatikow *et al.* 2006] S. Fatikow, T. Wich, H. Hülsen, T. Sievers and M. Jähnisch, "Microrobot system for automatic nanohandling inside a scanning electron microscope", *Proc. IEEE Int'l Conf. on Robotics & Automation (ICRA '06)*, Orlando, FL, pp. 1401-1407, May 15-19, 2006.

[Finch *et al.* 1995] M. Finch, V. L. Chi, R. M. Taylor II, M. Falvo, S. Washburn and R. Superfine, "Surface modification tools in a virtual environment interface to a scanning probe microscope", *Proc. ACM Symp. on Interactive 3D Graphics*, Monterey, CA, pp. 13-18, April 9-12, 1995.

[Garcia & San Paulo 1999] R. Garcia and A. San Paulo, "Attractive and repulsive tip-sample interaction regimes in tapping-mode atomic force microscopy", *Physical Review B*, Vol. 60, No. 7, pp. 4961-4967, 15 August 1999.

[Garcia & San Paulo 2000] R. Garcia and A. San Paulo, "Amplitude curves and operating regimes in dynamic atomic force microscopy", *Ultramicroscopy*, Vol. 82, Nos. 1-4, pp. 79-83, February 2000.

[Garno *et al.* 2003], J. C. Garno, Y. Yang, N. A. Amro, S. Cruchon-Dupeyrat, S. Chen and G.-Y. Liu, "Precise positioning of nanoparticles on surfaces using scanning probe lithography", *Nanoletters*, Vol. 3, No. 3, pp. 389-395, March 2003.

[Guthold *et al.* 2000] M. Guthold, M. R. Falvo, W. G. Matthews, S. Paulson, S. Washburn, D. A. Erie, R. Superfine, F. P. Brooks, Jr. and R. M. Taylor II, "Controlled manipulation of molecular samples with the nanoManipulator", *IEEE/ASME Trans. on Mechatronics*, Vol. 5, No. 2, pp. 189-198, June 2000.

[Harel *et al.* 2005] E. Harel, S. E. Meltzer, A. A. G. Requicha, M. E. Thompson and B. E. Koel, "Fabrication of latex nanostructures by nanomanipulation and thermal processing", *Nanoletters*, Vol. 5, No. 12, pp. 2624-2629, December 2005.

[Hertel *et al.* 1998] T. Hertel, R. Martel and Ph. Avouris, "Manipulation of individual carbon nanotubes and their interaction with surfaces", *J. Physical Chemistry B*, Vol. 102, No.6, pp. 910-915, 5 February 1998.

[Hollis *et al.* 1990] R. L. Hollis, S. Salcudean and D. W. Abraham, "Toward a tele-nanorobotic manipulation system with atomic scale force feedback and motion resolution", *Proc. IEEE Int'l Conf. on Microelectromechanical Systems*, Napa Valley, CA, pp. 115-119, February 11-14, 1990.

[Hsieh *et al.* 2002] S. Hsieh, S. Meltzer, C. R. C. Wang, A. A. G. Requicha, M. E. Thompson and B. E. Koel, "Imaging and manipulation of gold nanorods with an Atomic Force Microscope", *J. Physical Chemistry B*, Vol. 106, No. 2, pp. 231-234, January 17, 2002.

[Israelachvili 1992] J. N. Israelachvili, *Intermolecular and Surface Forces*. San Diego, CA: Academic Press, 1992, 2nd ed.

[Jung *et al.* 1996] T. A. Jung, R. R. Schlitter, J. K. Gimzewski, H. Tang and C. Joachim, "Controlled room-temperature positioning of individual molecules: molecular flexure and motion", *Science*, Vol. 271, No. 5246, pp. 181-184, 12 January 1996.

[Junno *et al.* 1995] T. Junno, K. Deppert, L. Montelius and L. Samuelson, "Controlled manipulation of nanoparticles with an atomic force microscope", *Applied Physics Letters*, Vol. 66, No. 26, pp. 3627-3629, 26 June 1995.

[Junno *et al.* 1988] T. Junno, S.-B. Carlsson, H. Xu, L. Montelius and L. Samuelson, "Fabrication of quantum devices by Ångström-level manipulation of nanoparticles with an atomic force microscope", *Applied Physics Letters*, Vol. 72, No. 5, pp. 548-550, 2 February 1998.

[Knuth 1993] D. E. Knuth, *The Stanford GraphBase*. New York, NY: The ACM Press, 1993.

[Latombe 1991] J.-C. Latombe, *Robot Motion Planning*. Boston, MA: Kluwer, 1991.

[Lewis & Ahmed 1999] P. A. Lewis and H. Ahmed, "Patterning of silicon nanopillars formed with a colloidal gold etch mask", *J. Vacuum Science & Technology B*, Vol. 17, No. 6, pp. 3239-3243, November/December 1999.

[Li *et al.* 2003a] G. Li, N. Xi, M. Yu and W. K. Fung, "Augmented reality system for real-time nanomanipulation", *Proc. IEEE Int'l Conf. on Nanotechnology*, S. Francisco, CA, pp. 64-67, August 12-14, 2003.

[Li *et al.* 2003b] G. Li, N. Xi, M. Yu and W. K. Fung, "3-D nanomanipulation using atomic force microscopy", *Proc. IEEE Int'l Conf. Robotics & Automation (ICRA '03)*, Taipei, Taiwan, pp. 3642-3647, September 14-19, 2003.

[Li *et al.* 2004] G. Li, N. Xi, M. Yu and W. K. Fung, "Development of augmented reality system for AFM-based nanomanipulation", *IEEE/ASME Trans. on Mechatronics*, Vol. 9, No. 2, pp. 358-365, June 2004.

[Lyo & Avouris 1991] I.-W. Lyo and Ph. Avouris, "Field-induced nanometer- to atomic-scale manipulation of silicon surfaces with the STM", *Science*, Vol. 253, No. 5016, pp. 173-176, 12 July 1991.

[Madsen *et al.* 2003] D. N. Madsen, K. Mølhave, R. Mateiu, P. Bøggild, A. M. Rasmussen, C. C. Appel, M. Brorson and C. J. H. Jacobsen, "Nanoscale soldering of positioned carbon nanotubes using highly conductive electron beam induced gold deposition", *Proc. IEEE Int'l Conf. on Nanotechnology*, S. Francisco, CA, pp. 335-338, August 12-14, 2003.

[Maier *et al.* 2001] S. A. Maier, M. L. Brongersma, P. G. Kik, S. Meltzer, A. A. G. Requicha, B. E. Koel and H. A. Atwater, "Plasmonics – a route to nanoscale optical devices", *Advanced Materials*, Vol. 13, No. 19, pp.1501-1505, October 2, 2001.

[Maier *et al.* 2003] S. A. Maier, P. G. Kik, H. A. Atwater, S. Meltzer, E. Harel, B. E. Koel and A. A. G. Requicha, "Local detection of electromagnetic energy transport below the diffraction limit in metal nanoparticle plasmon waveguides", *Nature Materials*, Vol. 2, No. 4, pp. 229-232, April 2003.

[Makaliwe & Requicha 2001] J. H. Makaliwe and A. A. G. Requicha , "Automatic planning of nanoparticle assembly tasks", *Proc. IEEE Int'l Symp. on Assembly & Task Planning (ISATP '01)*, Fukuoka, Japan, pp. 288-293, May 28-30, 2001.

[Mamin H. J. Mamin, P. H. Guethner and D. Rugar, "Atomic emission from a gold scanning-tunneling-microscope tip", *Physical Review Letters*, Vol. 65, No. 19, pp. 2418-2421, 5 November 1990.

[Martin *et al.* 1998] M. Martin, L. Roschier, P. Hakonen, U. Parts, M. Paalanen, B. Schleicher and E. I. Kauppinen, "Manipulation of Ag nanoparticles utilizing noncontact

atomic force microscopy”, *Applied Physics Letters*, Vol. 73, No. 11, pp. 1505-1507, September 14, 1998.

[Maruno *et al.* 1993] S. Maruno, K. Inanaga and T. Isu, “Threshold height for movement of molecules on Si(111)-7x7 with a scanning tunneling microscope”, *Applied Physics Letters*, Vol. 63, No. 10, pp. 1339-1341, 6 September 1993.

[Meltzer *et al.* 2001] S. Meltzer, R. Resch, B. E. Koel, M. E. Thompson, A. Madhukar, A. A. G. Requicha and P. Will, “Fabrication of nanostructures by hydroxylamine-seeding of gold nanoparticle templates”, *Langmuir*, Vol. 17, No. 5, pp. 1713-1718, March 6, 2001.

[Mesquida & Stemmer 2001] P. Mesquida and A. Stemmer, “Attaching silica nanoparticles from suspension onto surface charge patterns generated by a conductive atomic force microscope tip”, *Advanced Materials*, Vol. 13, No. 18, pp. 1395-1398, 14 September 2001.

[Meyer *et al.* 2004] E. Meyer, H. J. Hug and R. Bennewitz, *Scanning Probe Microscopy*. Heidelberg, Germany: Springer Verlag, 2004.

[Miyazaki & Sato 1997] H. Miyazaki and T. Sato, “Mechanical assembly of three-dimensional microstructures from fine particles”, *Advanced Robotics*, Vol. 11, No. 2, pp. 169-185, 1997.

[Mokaberi & Requicha 2004] B. Mokaberi and A. A. G. Requicha, “Towards automatic nanomanipulation: drift compensation in scanning probe microscopy”, *Proc. IEEE Int’l Conf. on Robotics & Automation (ICRA ‘04)*, New Orleans, LA, pp. 416-421, April 25-30, 2004.

[Mokaberi & Requicha 2006] B. Mokaberi and A. A. G. Requicha, “Drift compensation for automatic nanomanipulation with scanning probe microscopes”, Vol. 3, No. 3, pp. 199-207, July 2006.

[Mokaberi & Requicha 2007] B. Mokaberi and A. A. G. Requicha, “Compensation of scanner creep and hysteresis for AFM nanomanipulation”, *IEEE Trans. on Automation Science & Engineering*, in press.

[Mokaberi *et al.* 2007] B. Mokaberi, J. Yun, M. Wang and A. A. G. Requicha, “Automated nanomanipulation with atomic force microscopes”, *Proc. IEEE Int’l Conf. on Robotics & Automation (ICRA ‘07)*, Rome, Italy, pp. 1406-1412, April 10-14, 2007.

[Piner *et al.* 1999] R. D. Piner, J. Zhu, F. Xu, S. Hong and C. A. Mirkin, “Dip-Pen Nanolithography”, *Science*, Vol. 283, No. 5402, pp. 661-663, 29 January 1999.

[Requicha *et al.* 1998] A. A. G. Requicha, C. Baur, A. Bugacov, B. C. Gazen, B. Koel, A. Madhukar, T. R. Ramachandran, R. Resch and P. Will, “Nanorobotic assembly of two-

dimensional structures”, *Proc. IEEE Int’l Conf. on Robotics & Automation (ICRA ‘98)*, Leuven, Belgium, pp. 3368-3374, May 16-21, 1998.

[Requicha 1999a] A. A. G. Requicha, “Massively parallel nanorobotics for lithography and data storage”, *Int’l J. Robotics Research*, Vol. 18, No. 3, pp. 344-350, March 1999.

[Requicha 1999b] A. A. G. Requicha, “Nanoparticle Patterns”, *J. Nanoparticle Research*, Vol. 1, No. 3, pp. 321-323, September 1999.

[Requicha *et al.* 1999] A. A. G. Requicha, R. Resch, N. Montoya, B. E. Koel, A. Madhukar and P. Will, “Towards hierarchical nanoassembly”, *Proc. Int’l Conf. on Intelligent Robots and Systems (IROS ‘99)*, Kyongju, S. Korea, pp. 889-893, October 17-21, 1999.

[Requicha *et al.* 2001] A. A. G. Requicha, S. Meltzer, P. F. Terán Arce, J. H. Makaliwe, H. Sikén, S. Hsieh, D. Lewis, B. E. Koel and M. E. Thompson, “Manipulation of nanoscale components with the AFM: principles and applications”, *Proc. 1st IEEE Int’l Conf. on Nanotechnology*, Maui, HI, pp. 81-86, October 28-30, 2001.

[Requicha 2003] A. A. G. Requicha, “Nanorobots, NEMS and nanoassembly”, *Proc. IEEE*, special issue on nanoelectronics and nanoscale processing, Vol. 91, No. 11, pp. 1922-1933, November 2003.

[Resch *et al.* 1998a] R. Resch, A. Bugacov, C. Baur, B. E. Koel, A. Madhukar, A. A. G. Requicha and P. Will, “Manipulation of nanoparticles using dynamic force microscopy: simulation and experiments”, *Applied Physics A*, Vol. 67, No. 3, pp. 265-271, September 1998.

[Resch *et al.* 1998b] R. Resch, C. Baur, A. Bugacov, B. E. Koel, A. Madhukar, A. A. G. Requicha and P. Will, “Building and manipulating 3-D and linked 2-D structures of nanoparticles using scanning force microscopy”, *Langmuir*, Vol. 14, No. 23, 10 November 1998.

[Resch *et al.* 1999] R. Resch, C. Baur, A. Bugacov, B. E. Koel, P. M. Echternach, A. Madhukar, N. Montoya, A. A. G. Requicha and P. Will, “Linking and manipulation of gold multi-nanoparticle structures using dithiols and scanning force microscopy”, *J. Physical Chemistry B*, Vol. 103, No. 18, pp. 3647-3650, 6 May 1999.

[Resch *et al.* 2000] R. Resch, D. Lewis, S. Meltzer, N. Montoya, B. E. Koel, A. Madhukar, A. A. G. Requicha and P. Will, “Manipulation of gold nanoparticles in liquid environments using scanning force microscopy”, *Ultramicroscopy*, Vol. 82, Nos. 1-4, pp. 135-139, February 2000.

[Resch *et al.* 2001] R. Resch, S. Meltzer, T. Vallant, H. Hoffmann, B. E. Koel, A. Madhukar, A. A. G. Requicha and P. Will, “Immobilizing Au nanoparticles on SiO₂

surfaces using octadecylsiloxane monolayers”, *Langmuir*, Vol. 17, No. 18, pp. 5666-5670, 4 September 2001.

[Roschier *et al.* 1999] L. Roschier, J. Penttilä, M. Martin, P. Hakonen, M. Paalanen, U. Tapper, E. Kauppinen, C. Journet and P. Bernier, “Single-electron transistor made of multi-walled carbon nanotube using scanning probe manipulation”, *Applied Physics Letters*, Vol. 75, No. 5, pp. 728-730, 2 August 1999.

[Salling & Lagally 1994] C. T. Salling and M. G. Lagally, “Fabrication of atomic-scale structures on Si(001) surfaces”, *Science*, Vol. 265, No. 5171, pp. 502-506, 22 July 1994.

[Sarid 1994] S. Sarid, *Scanning Force Microscopy*. Oxford, U.K.: Oxford University Press, 1994.

[Sato *et al.* 1995] T. Sato, T. Kameya, H. Miyazaki and Y. Hatamura, “Hand-eye system in the nano manipulation world”, *Proc. IEEE Int’l Conf. on Robotics & Automation*, Nagoya, Japan, pp. 59-66, May 21-27, 1995.

[Schaefer *et al.* 1995] D. M. Schaefer, R. Reifenberger, A. Patil and R. P. Andres, “Fabrication of two-dimensional arrays of nanometer-size clusters with the atomic force microscope”, *Applied Physics Letters*, Vol. 66, No. 8, pp. 1012-1014, 20 February 1995.

[Sheehan & Lieber 1996] P. E. Sheehan and C. M. Lieber, “Nanotribology and nanofabrication of MoO₃ structures by atomic force microscopy”, *Science*, Vol. 272, No. 5265, pp. 1158-1161, 24 May 1996.

[Sitti & Hashimoto 1998] M. Sitti and H. Hashimoto, “Tele-nanorobotics using atomic force microscope”, *Proc. IEEE/RSJ Int’l. Conf. on Intelligent Robots & Systems (IROS ’98)*, Victoria, Canada, pp. 1739-1746, October 13-17, 1998.

[Sitti & Hashimoto 2000] M. Sitti and H. Hashimoto, “Controlled pushing of nanoparticles: modeling and experiments”, *IEEE/ASME Trans. on Mechatronics*, Vol. 5, No. 2, pp. 199-211, June 2000.

[Snow & Campbell 1995] E. S. Snow and P. M. Campbell, *Science*, Vol. 270, pp. 1639-1641, 8 December 1995.

[Stroscio & Eigler 1991] J. A. Stroscio and D. M. Eigler, “Atomic and molecular manipulation with the scanning tunneling microscope”, *Science*, Vol. 254, No. 5036, pp. 1319-1326, 29 November 1991.

[Stroscio *et al.* 2006] J. A. Stroscio, F. Tavazza, J. N. Crain, R. J. Celotta and A. M. Chaka, “Electronically-induced atom motion in engineered CoCu_n nanostructures”, *Science*, Vol. 313, No. 5789, pp. 948-951, 18 August 2006.

[Sun & Legget 2002] S. Sun and G. J. Legget, "Generation of nanostructures by scanning near-field photolithography of self-assembled monolayers and wet chemical etching", *Nanoletters*, Vol. 2, No. 11, pp. 1223-1227, November 2002.

[Tada *et al.* 1998] T. Tada, T. Kanayama, K. Koga, K. Seeger, S. J. Carroll, P. Weibel and R. E. Palmer, "Fabrication of size-controlled 10-nm scale Si pillars using metal clusters as formation nuclei", *Microelectronic Engineering*, Vol. 41/42, pp. 539-542, March 1998.

[Takeda *et al.* 2003] S. Takeda, C. Nakamura, C. Miyamoto, N. Nakamura, M. Kageshima, H. Tokumoto and J. Miyake, "Lithographing of biomolecules on a substrate surface using an enzyme-immobilized AFM tip", *Nanoletters*, Vol. 3, No. 11, pp. 1471-1474, November 2003.

[Taylor *et al.* 1993] R. M. Taylor II, W. Robinett, V. L. Chi, F. P. Brooks, Jr., W. V. Wright, R. S. Williams and E. J. Snyder, "The nanomanipulator: a virtual reality interface for a scanning tunneling microscope", *Proc. ACM SIGGRAPH '93*, Anaheim, CA, pp. 127-134, August 1-6, 1993.

[Taylor *et al.* 1997] R. M. Taylor II, J. Chen, S. Okimoto, N. Llopis-Artime, V. L. Chi, F. P. Brooks, Jr., M. Falvo, S. Paulson, P. Thiansathaporn, D. Glick, S. Washburn and R. Superfine, "Pearls found on the way to the ideal interface for scanned-probe microscopes", *Proc. IEEE Visualization '97*, Phoenix, AZ, pp. 467-470, October 19-24, 1997.

[Theil Hansen *et al.* 1998] L. Theil Hansen, A. Kühle, A. H. Sørensen, J. Bohr and P. E. Lindelof, "A technique for positioning nanoparticles using an atomic force microscope", *Nanotechnology*, Vol. 9, No. 4, pp. 337-342, December 1998.

[Uchida *et al.* 1993] H. Uchida, D. H. Huang, J. Yoshinobu and M. Aono, "Single atom manipulation on the Si(111)7x7 surface by the scanning tunneling microscope (STM)", *Surface Science*, Vols. 287/288, Part 2, pp. 1056-1061, 10 May 1993.

[Vettiger *et al.* 2002] P. Vettiger, G. Cross, M. Despont, U. Drechsler, U. Dürig, B. Gotsmann, W. Häberle, M. A. Lantz, H. E. Rothuizen, R. Stutz, G. K. Binnig, "The "millipede" - nanotechnology entering data storage", *IEEE Trans. on Nanotechnology*, Vol. 1, No. 1, pp. 39-55, March 2002.

[Vikramaditya & Nelson 1997] B. Vikramaditya and B. J. Nelson, "Visually guided microassembly using optical microscopes and active vision", *Proc. IEEE Int'l Conf. on Robotics & Automation*, Albuquerque, NM, pp. 3172-3177, April 21-27, 1997.

[Villarrubia 1994] J. S. Villarrubia, "Morphological estimation of tip geometry for scanned probe microscopy", *Surface Science*, Vol. 321, No. 3, pp. 287-300, 20 December 1994.

[Wiesendanger 1994] R. Wiesendanger, *Scanning Probe Microscopy and Spectroscopy*. Cambridge, U.K.: Cambridge University Press, 1994, Chapter 8.

[Wouters & Schubert 2004] D. Wouters and U. S. Schubert, “Nanolithography and nanochemistry: probe-related patterning techniques and chemical modification for nanometer-sized devices”, *Angewandte Chemie Int'l Ed.*, Vol. 43, No. 19, pp. 2480-2495, 3 May 2004.

[Yu *et al.* 1999] M.-F. Yu, M. J. Dyer, G. D. Skidmore, H. W. Rohrs, X.-K. Lu, K. D. Hausman, J. R. von Her and R. S. Ruoff, “Three dimensional manipulation of carbon nanotubes under a scanning electron microscope”, *Nanotechnology*, Vol. 10, No. 3, pp. 244-252, September 1999.

[Zheng *et al.* 2000] J. Zheng, Z. Chen, and Z. Liu, “Atomic force microscopy-based nanolithography on silicon using colloidal Au nanoparticles as a nanooxidation mask”, *Langmuir*, Vol. 16, No. 24, pp. 9673-9676, 28 November 2000.